

**Studying the Effect of the ROCK Inhibitor on the  
Proliferation Potential of Human Induced Pluripotent Stem  
Cells under 2D/3D and Static/Dynamic Culture  
Environments**

**Mafalda Gomes Pereira**

Thesis to obtain the Master of Science Degree in

**Biological Engineering**

Supervisor: Professor Masahiro KINO-OKA

Supervisor: Professor Cláudia Alexandra Martins Lobato da Silva

**Examination Committee**

Chairperson: Professor Maria Ângela Cabral Garcia Taipa Meneses de Oliveira

Supervisor: Professor Cláudia Alexandra Martins Lobato da Silva

Member of the Committee: Doctor Cláudia Daniela Canelas Miranda

**November 2018**



# ACKNOWLEDGMENTS

To my family, my friends and everyone else who has contributed, directly or indirectly, not only for the development of this thesis, but also throughout my whole academic years.

Firstly, I would like to thank Kino-oka sensei, who did not hesitate in accepting me into his laboratory at Osaka University. Thank you very much for this incredible opportunity of doing my research work at your laboratory. Not only I learned so much through the experiments, but I also felt integrated into a team. Also, thank you very much for always being so fond of my interests and constantly motivate me to travel and explore more of Japan and learn more about the Japanese culture.

I would like to thank also to Yamamoto Riku san, for the endless patient and enlightening tutoring that lasts up until now. Besides all the advice you gave me, I would like to thank you for the time spent at the laboratory, where I learned and improved my technique. Also, thank you for introducing me to the habits and traditions of the laboratory. You were more than just a tutor, you were also a friend.

Also, I would like to thank Horiguchi sensei, for the time he spent advising me and suggesting improvements in my work.

I would also like to thank very much to Nishimura san, who made my travel preparations and arrival to Japan so smooth, without any issues at all, and for the constant help the following months, also with the help of Wakamatsu san.

Of course, I would like to thank all the laboratory members, both Japanese and international students, who made me feel so welcomed since the very first day. I believe we have created some strong bonds with each other and you alone made my journey unforgettable. Thank you for all the help at the laboratory and the data you provided me with for the elaboration of this thesis, but, especially, thank you very much for all Japanese lessons, the laughter, the thoughts and the experiences we shared together. I learned so much with all of you. 皆さん、ありがとうございます！またね！（Everyone, thank you very much! See you!).

Back in Portugal, firstly, I would like to thank Professor Cláudia Lobato da Silva, not only for cultivating in me the curiosity for this theme in previous subjects of the course, but also for her advice and help in the realization of this thesis. Your constant availability and, most importantly, your genuine sympathy made this work easier to accomplish.

Secondly, I would like to thank Doctor Cláudia Miranda, for the initial advice about the thesis and the chance of following part of her work at Taguspark.

Also, thank you to my professors who accompanied my academic journey for all these years.

I want to thank all my friends, who supported me so much since ever, and even when I was 8 time zones and over 11000 kilometers away from home.

To my “Técnico friends”, with whom I have faced the course’s adversities and who helped me so much since day one. Técnico might be tough, but every studying session, group project, presentation

or last-minute questions were so much peaceful since I could always trust on you and laugh together with you. Thank you so much for your everlasting friendship.

Of course, thank you to my high school friends, and to those who have been with me since ever and practically grew up with me. I apologise for all the moments I was absent because of deadlines I had to meet. We might have gone separate ways after the high school years, but we still meet and talk frequently as if we see each other every day. I truly thank you for the amazing friendship for all these years and still counting.

And last, but definitely not least, to my family, especially to my parents, who have loved me unconditionally and were there for me in every moment of my life, in my disappointments and failures, but also in my victories and euphoria moments, whenever and wherever. Thank you so much for supporting my ideas and motivate even more my will to travel, to explore and to challenge myself.

My true words cannot entirely express my feelings towards all the love, support and help you have given me, but please accept these humble acknowledgments. From the bottom of my heart: thank you so much. I am dedicating this thesis to all of you.



# ABSTRACT

Human induced pluripotent stem cells (hiPSCs) have unlimited self-renewal properties and the capacity to give rise to cells from the three embryonic germ layers. The clinical potential of these cells has brought to light promising work for future applications, though having fully defined protocols for their maintenance and handling, under good manufacturing practices (GMP), is still a universal challenge.

In this work, two stocks of hiPSCs from the same line (1383D2) were compared, since one of the stocks had displayed significant phenotypical changes. The contribution of the ROCK inhibitor was studied in 2D culture for 24 hours, and in 3D static and dynamic cultivation, for 48 hours and 96 hours. In 2D culture, the growth kinetics for both stocks showed to be similar. However, in 3D dynamic culture, the live cell ratio for the altered cells was not higher than 0.20, when comparing to the other stock ( $0.67 \pm 0.04$ ). Though, the apparent specific growth rate was overall much higher in these cells, the highest being  $3.57 \times 10^{-2} \text{ h}^{-1}$ , achieved in 3D static culture, exposed to the ROCK inhibitor for 96 hours. Naturally, the largest aggregates (assessed by the aggregates' diameter) were obtained in dynamic culture. Furthermore, for the study of the morphology and viability of the aggregates, the expression of E-cadherin and Ki-67 were also analysed, showing that larger aggregates suffered central necrosis as the culture proceeded. Nevertheless, despite the differences, the present results permitted to conclude that these altered cells are possibly viable for future use.

**Keywords:** Human induced pluripotent stem cells; ROCK inhibitor; Static Culture; Dynamic Culture; Growth kinetics; Aggregate development.

# RESUMO

Células estaminais pluripotentes induzidas humanas (hiPSCs) têm propriedades de autorrenovação ilimitada e a capacidade de originarem células das três camadas germinativas embrionárias. O potencial clínico destas células possibilitou o desenvolvimento de trabalho promissor para aplicações futuras, contudo ter protocolos completamente definidos para a sua manutenção e manuseamento, mantendo boas práticas de fabricação (GMP), é ainda um desafio universal.

Neste trabalho, dois *stocks* de hiPSCs da mesma linha (1383D2) foram comparados, visto que um deles demonstrou ter mudanças fenotípicas significativas. A contribuição do inibidor ROCK foi estudada em cultura 2D por 24 horas, e em cultura 3D estática e dinâmica, por 48 horas e 96 horas. Em cultura 2D, a cinética de crescimento para os dois tipos de *stocks* mostrou ser semelhante. Contudo, em cultura 3D dinâmica, o rácio de células vivas para as células alteradas não foi superior a 0.20, quando comparando com o outro *stock* ( $0.67 \pm 0.04$ ). Já a taxa de crescimento específico aparente foi globalmente muito superior nestas células, sendo a mais elevada de  $3.57 \times 10^{-2} \text{ h}^{-1}$ , alcançada em cultura 3D estática, exposta ao inibidor ROCK por 96 horas. Naturalmente, os agregados maiores (avaliados através do diâmetro dos agregados) foram obtidos em cultura dinâmica. Todavia, para o estudo da morfologia e viabilidade dos agregados, a expressão de E-caderina e Ki-67 foi também analisada, que mostrou que agregados maiores sofrem necrose central com o progresso da cultura. Não obstante, apesar das diferenças, os presentes resultados permitiram concluir que estas células alteradas estão possivelmente viáveis para uso futuro.

**Palavras-chaves:** Células estaminais pluripotentes induzidas humanas; Inibidor ROCK; Cultura estática; Cultura dinâmica; Cinética de crescimento; Desenvolvimento de agregados.

# LIST OF CONTENTS

ACKNOWLEDGMENTS .....	3
ABSTRACT .....	6
RESUMO .....	7
LIST OF CONTENTS .....	8
LIST OF FIGURES .....	10
LIST OF TABLES .....	13
LIST OF ABBREVIATIONS .....	14
1. INTRODUCTION .....	16
1.1. Human Pluripotent Stem Cells .....	16
1.1.1 Human Embryonic Stem Cells.....	17
1.1.2. Human Induced Pluripotent Stem Cells .....	18
1.2. Applications of Human Pluripotent Stem Cells .....	20
1.3. Expansion of Human Pluripotent Stem Cells .....	23
1.3.1. Xeno-free, Feeder-free and Chemically Defined Culture Systems .....	23
1.3.2. Process Standardization.....	24
1.3.3. Passaging of Human Pluripotent Stem Cells .....	26
1.3.3.1. EDTA and Trypsin in Cell Passaging.....	27
1.3.3.2. ROCK Inhibitor .....	27
1.3.4. Large-scale Expansion of Human Pluripotent Stem Cells .....	28
1.3.4.1. Platforms for Large-scale Expansion of hPSCs.....	29
1.3.4.2. Microcarrier-based 3D Dynamic Suspension Cultures .....	32
1.3.4.3. Aggregate-based 3D Cultures .....	34
1.3.4.3.1. Aggregate-based 3D Static Cultures .....	35
1.3.4.3.2. Aggregate-based 3D Dynamic Cultures .....	36
2. AIM OF THE STUDIES .....	39
3. MATERIALS AND METHODS .....	40
3.1. Cell Culture .....	40
3.1.1. Cell line .....	40
3.1.2. Culture media .....	40
3.2. Culture Preparation .....	40
3.2.1. Cells' Maintenance .....	40
3.2.2. Cells' Harvesting and Passaging.....	41
3.2.3. Cells' Counting .....	41
3.2.4. Culture Inoculation.....	42
3.2.4.1. 2D Static Conditions .....	42



3.2.4.2. 3D Static Conditions .....	42
3.2.4.3. 3D Dynamic Conditions .....	43
3.3. Cryopreservation .....	43
3.4. Aggregates' Sectioning.....	44
3.5. Characterization of hiPSCs .....	44
3.5.1. Attachment Efficiency and Live Cell Ratio.....	44
3.5.2. Specific Growth Rate and Apparent Specific Growth Rate .....	45
3.5.3. Aggregates' Diameter.....	45
3.5.4. Aggregates' Morphology.....	46
3.5.5. Immunostaining .....	46
4. RESULTS AND DISCUSSION.....	48
4.1. hiPSCs' Divergence.....	48
4.2. Culturing in 2D Environment.....	49
4.3. Effect of the Exposure to ROCK Inhibitor.....	52
4.3.1. Influence of Exposure Time to ROCK Inhibitor .....	52
4.3.2. Static and Dynamic Conditions .....	55
4.3.3. Aggregates' Morphology.....	58
5. CONCLUSIONS AND FUTURE PERSPECTIVES .....	65
REFERENCES .....	67
ANNEXES.....	75

# LIST OF FIGURES

**Figure 1 - Characteristics of embryonic stem cells.** (Adapted from Winslow, T. in *Regenerative Medicine*, 2006)<sup>5</sup>. ..... 18

**Figure 2 - Skin cells can be reprogrammed into iPSC cells that can then develop into different types of cells.** (Credit to Sanger Institute, Genome Research Limited, removed from <https://www.sanger.ac.uk/news/view/scientists-unveil-uk-s-largest-resource-human-stem-cells-healthy-donors>, accessed on 01/10/2018). ..... 19

**Figure 3 – Roadblocks to translating human iPSC technology to the clinic.** Human iPSCs technology potentially can be used for screening new cancer drugs (blue box) and ultimately for providing cells for transplant to treat a variety of diseases, including cancer (yellow box). Genetic mutations can be corrected in patient-derived iPSCs by gene targeting approaches. The main hurdles to using patient-specific iPSCs for disease modelling, drug screening, and transplantation purposes are **(i)** a lack of effective differentiation protocols, **(ii)** little or no engraftment capability for the majority of human iPSC-derived specialized cells, **(iii)** difficulties in modelling multifactorial diseases, **(iv)** the need for GMP-compliant conditions at each step, and **(v)** safety concerns regarding the potential tumorigenicity of iPSCs associated with their pluripotent state or with insertional or culture-driven mutagenesis. Dotted arrow not yet tested; solid arrow, only a few studies available; blue arrow, feasible but requires further study. (Adapted from Sharkis et al.<sup>33</sup>, National Institute of Health Public Access).21

**Figure 4 – Process flowchart for cGMP manufacturing of hPSC-based therapeutic products and critical quality parameters related to each step of processing.** The process flowchart is divided into **(A)** cell line development and banking and **(B)** cGMP manufacturing sections. In the cell line development and banking section, clinical grade hPSCs are produced using safe derivation or reprogramming technologies, which have been characterized after their maintenance in xeno-free and fully defined conditions before cryopreservation in master cell banks to be used as the main starting material for cGMP manufacturing. The cGMP manufacturing process is divided into three main processing stages including upstream processing, downstream processing, and delivery or storage. In upstream processing, hPSCs are expanded and differentiated to targeted cell therapeutic products. The targeted cell products are isolated and purified, formulated and/or filled for instant or delayed delivery. In the delivery or storage stage, the therapeutic cell products are handled and transferred to the final user or patient or preserved in large working cell banks for delayed delivery. A robust quality control (QC) and quality assurance (QA) system will control and monitor the whole manufacturing process based on critical quality parameters in each processing step. (Adapted from Abbasalizadeh *et al.*<sup>53</sup>). 25

**Figure 5 – Discovery of the method for suppressing loss of dispersed human ES cell viability with the use of the ROCK inhibitor.** (Removed from [https://www.mst.or.jp/portals/0/prize/english/winners/bio/bio2012\\_en.html](https://www.mst.or.jp/portals/0/prize/english/winners/bio/bio2012_en.html), accessed on 18/09/2018, based on the works of Watanabe et al.<sup>59</sup> and Ohgushi et al.<sup>66</sup>). ..... 28

**Figure 6 - Platforms for large-scale expansion of hPSCs.** (A) Comparison of the various platforms and their properties; (B) 2D static T-flask-based cultures are scaled out, adding more layers and enlarging the culturing surface. In the Xpansion® (ATMI) system, continuous media change and online monitoring are available; (C) 3D-aggregate culturing on orbital shakers is suitable for process development and small-scale protocol optimization; (D) Spinner flasks can act as a preliminary step before moving to a stirred-tank bioreactor because the agitation techniques are similar. However, the system is not monitored and does not allow continuous media change; (E) Rotary cell culture system is suitable for small-scale optimization of hPSC expansion and differentiation; (F) Cell culture bags are applicable for GMP manufacturing. They are single-use and equipped with online sensors and a perfusion system; (G) Stirred-tank bioreactors are widely used and easily scaled up. They are extremely flexible and suitable for multiple applications, enabling continuous media change and online control and monitoring of culture parameters. (Adapted from Lavon et al.<sup>67</sup>). ..... 31

**Figure 7 - Morphology of various types of microcarriers (MCs).** (A) Glass (SoloHill) MCs as spherical beads; (B) Cytodex-3 as spherical beads; (C) Fibra-Cel® with porous microfibers; (D) Synthemax® II MCs with vitronectin peptide acrylate surface; (E) rat cartilage MSCs grown on CultiSpher-S; (F) PSC-derived extracellular matrix MCs. (Scale bars = 100 µm, adapted from Sart et al.<sup>86</sup>). ..... 33

**Figure 8 - Illustration of a bioprocess engineering approach with bioreactors to alleviate current limitations in the use of stem cells for clinical application.** Bioreactors enable the large-scale stem cell expansion and differentiation in a controlled environment. They also allow to control the mechanical forces, feeds, and gradients of nutrients and growth factors, pH, oxygen, as well as the aggregate size. With the detailed characterizations of input cells and output cells, the homogeneity of the produced cell population will be increased. (Adapted from Sart et al.<sup>97</sup>). ..... 37

**Figure 9 - Overall design of the experiment.** hiPSCs were cultured in 2D static environment, using 8-well plates, with a culture time of 120 hours and ROCK inhibitor in the culture for 24 hours. .... 48

**Figure 10 – Overall design of the experiment.** hiPSCs were cultured in 3D static and dynamic environment, using 6-well dimple plates and 30 mL bioreactors, respectively, for a culture time of 96 hours and ROCK inhibitor in the culture for 48 and 96 hours. .... 49

**Figure 11 - Images captured using phase contrast microscope of hiPSC for Type A cells.** Images were taken at (A)  $t = 24$  h, (B)  $t = 72$  h and (C)  $t = 120$  h. Dead cells correspond to the yellow floating spheres ( $n = 1$ ). (Scale bars = 500 µm). ..... 50

**Figure 12 - Growth curve for the Type A culture in 2D static conditions.** The graphic was plotted using a semi-logarithmic scale on the y-axis, at  $t = 24$  h,  $t = 72$  h and  $t = 120$  h. The error bars represent the standard deviation ( $n = 3$ ). ..... 50

**Figure 13 - Variation of Type B cells' density in both 3D static and dynamic cultures with different exposure times to the ROCK inhibitor.** Graphic plotted in a semi-logarithmic scale on the y-axis at seeding time ( $t = 0$ ),  $t = 24$  h and  $t = 96$  h, for the condition of study of the effect of ROCK inhibitor in the culture for 48 hours and 96 hours ( $n = 1$ ). ..... 53

**Figure 14 - Variation of the aggregates' diameter.** Data collected at  $t = 24$  h, in both 3D static and dynamic culture, for the conditions of study of the effect of ROCK inhibitor in the culture for 48 hours and 96 hours ( $n = 1$ ). ..... 54

**Figure 15 - Variation of the aggregates' diameter.** Data collected using at  $t = 96$  h, in both 3D static and dynamic culture, for the conditions of study of the effect of ROCK inhibitor in the culture for 48 hours and 96 hours ( $n = 1$ ). ..... 54

**Figure 16 - Phase contrast microscope images of aggregates composed of Type B cells in the dimple plate.** These images were taken at  $t = 96$  h, with the ROCK inhibitor present in the culture for 48 hours in **(A)** and **(B)** and for 96 hours in **(C)** and **(D)** ( $n = 1$ ). (Scale bars = 200  $\mu\text{m}$ ). ..... 58

**Figure 17 – Phase contrast microscope images of aggregates composed of Type B cells from the culture 3D static culture, in dimple plates, and 3D dynamic culture, in 30 mL bioreactors.** These images were taken at  $t = 96$  h, showing the aggregates obtained from 3D static culture, with the ROCK inhibitor present in the culture for **(A)** 48 hours and **(B)** 96 hours, and obtained from 3D dynamic culture, with the ROCK inhibitor present in the culture also for **(C)** 48 hours and **(D)** 96 hours ( $n = 1$ ). (Scale bars = 200  $\mu\text{m}$ ). ..... 59

**Figures 18 - Immunostaining images of Type B cells, cultured in a 30 mL bioreactor operating for 96 hours, with the ROCK inhibitor in the culture for 48 hours.** The images represent the expression of **(A)** DAPI, **(B)** Ki-67, **(C)** E-cadherin and **(D)** the merge of the three late results ( $n = 1$ ). (Scale bars = 100  $\mu\text{m}$ ). ..... 61

**Figure 19 - Immunostaining images of Type B cells, cultured in a 30 mL bioreactor operating for 96 hours, with the ROCK inhibitor in the culture for 48 hours.** The images represent the expression of **(A)** DAPI, **(B)** Ki-67, **(C)** E-cadherin and **(D)** the merge of the three late results ( $n = 1$ ). (Scale bars = 100  $\mu\text{m}$ ). ..... 62

**Figure 20 - Images captured using phase contrast microscope of hiPSC, Type B cells.** Images were taken at **(A)**  $t = 24$  h, **(B)**  $t = 72$  h and **(C)**  $t = 120$  h. Dead cells correspond to the yellow floating spheres. These unpublished results were kindly provided by a laboratory member ( $n = 1$ ). (Scale bars = 500  $\mu\text{m}$ ). ..... 75

**Figure 21 - Phase contrast microscopy images of aggregates composed of Type A cells from the culture in a 30 mL bioreactor.** These images were taken at  $t = 24$  h, with the ROCK inhibitor present in the culture for **(A)** 24 hours and **(B)** 120 hours, and at  $t = 120$  h, with the ROCK inhibitor present in the culture also for **(C)** 24 hours and **(D)** 120 hours. These unpublished results were kindly provided by a laboratory member ( $n = 1$ ). (Scale bars = 200  $\mu\text{m}$ ). ..... 77

# LIST OF TABLES

<b>Table 1 - Examples of clinical trials using human embryonic stem cells (hESCs) and induced pluripotent stem cells (iPSCs).</b> Clinical trials as from 2016. RPE – retinal pigment epithelium (adapted from Trounson A. et al. <sup>34</sup> ). .....	22
<b>Table 2 - Primary antibodies' information regarding the type of host, clonality, reactivity, catalogue identity and supplier and working dilution.</b> .....	47
<b>Table 3 – Targeted primary antibodies' information regarding the type of host, clonality, reactivity, catalogue identity and supplier and working dilution.</b> .....	47
<b>Table 4 – Growth kinetics parameters, the attachment efficiency (<math>\alpha</math>) and the specific growth rate (<math>\mu</math>), for Type A and Type B cells, in 2D static culture.</b> The values represented are the average at $t = 24$ h and $t = 120$ h, respectively, for the condition of study of the effect of the ROCK inhibitor in the culture for 24 hours, followed by the standard deviation ( $\pm$ ). Type B cells' unpublished results were kindly provided by laboratory members ( $n = 1$ ). .....	51
<b>Table 5 - Growth kinetics parameters, the live cell ratio (<math>\alpha^*</math>) and the apparent specific growth rate (<math>\mu^{APP}</math>), for Type A and Type B cells, in 3D static and dynamic culture.</b> The values represented were collected at $t = 24$ h and $t = 96$ h, for the condition of study of the effect of ROCK inhibitor in the culture for 48 hours and 96 hours. Type A cell's results for 3D dynamic culture with the ROCK inhibitor for 48 hours are followed by the standard deviation ( $\pm$ ). Type A cells' unpublished results were kindly provided by the laboratory members ( $n = 1$ ). .....	56
<b>Table 6 – Growth kinetics parameters for the hiPS cells 2D static culture in 8-well plates for Type A cells, for attachment efficiency (<math>\alpha</math>) and specific growth rate (<math>\mu</math>).</b> The values represented are the average at $t = 24$ h and $t = 120$ h, respectively, for the condition of study of the effect of the ROCK inhibitor in the culture for 24 hours, followed by the standard deviation ( $\pm$ ). These unpublished results were kindly provided by laboratory members ( $n = 1$ ). .....	75
<b>Table 7 - Results from the Type A cells in 3D dynamic culture for the live cell ratio (<math>\alpha^*</math>) and apparent specific growth rate (<math>\mu^{APP}</math>).</b> The values represented are the average, followed by the standard deviation ( $\pm$ ), for the culture time of 120 h, for the condition of study of the effect of ROCK inhibitor in the culture for 24 hours and 120 hours. These unpublished results were kindly provided by a laboratory member ( $n = 1$ ). .....	76
<b>Table 8 - Results from the Type A cells in 3D static culture for the live cell ratio (<math>\alpha^*</math>) and apparent specific growth rate (<math>\mu^{APP}</math>).</b> The values represented are the average, followed by the standard deviation ( $\pm$ ), for the culture time of 120 h, for the condition of study of the effect of ROCK inhibitor in the culture for 24 hours. These unpublished results were kindly provided by laboratory members ( $n = 1$ ). .....	76

# LIST OF ABBREVIATIONS

<b>2D</b>	Two-dimensional
<b>3D</b>	Three-dimensional
<b>ASC</b>	Adipose-derived Stem Cells
<b>ATP</b>	Adenosine Triphosphate
<b>CAMs</b>	Cell Adhesion Molecules
<b>cGMP</b>	Current Good Manufacturing Practices
<b>CiRA</b>	Center for Induced Pluripotent Stem Cell Research and Application
<b>DAPI</b>	4',6-diamidino-2-phenylindole
<b>DNA</b>	Deoxyribonucleic Acid
<b>DPBS</b>	Dulbecco's Phosphate-buffered Saline
<b>EB</b>	Embryonic Bodies
<b>ECM</b>	Extracellular Matrix
<b>EDTA</b>	Ethylenediamine Tetraacetic Acid
<b>ESCs</b>	Embryonic Stem Cells
<b>FBS</b>	Fetal Bovine Serum
<b>FGF</b>	Fibroblast Growth Factor
<b>GABA</b>	<i>Gamma</i> -Aminobutyric Acid
<b>GMP</b>	Good Manufacturing Practices
<b>GTP</b>	Guanosine Triphosphate
<b>hESCs</b>	Human Embryonic Stem Cells
<b>hiPSCs</b>	Human Induced Pluripotent Stem Cells
<b>hPSCs</b>	Human Pluripotent Stem Cells
<b>iPSCs</b>	Induced Pluripotent Stem Cells
<b>MC</b>	Microcarriers
<b>MCB</b>	Master Cell Bank
<b>mEBs</b>	Mouse Embryonic Stem Cells
<b>MEF</b>	Mouse Embryonic Fibroblasts
<b>mESCs</b>	Mouse Embryonic Stem Cells

<b>MYH</b>	Myosin II Heavy Chains
<b>OCT</b>	Octamer-binding Transcription Factor
<b>PBS</b>	Phosphate-buffered Saline
<b>PDMS</b>	Poly(dimethylsiloxane)
<b>PEG</b>	Poly(ethylene glycol)
<b>PSCs</b>	Pluripotent Stem Cells
<b>QA</b>	Quality Assurance
<b>QC</b>	Quality Control
<b>ROCK</b>	Rho-associated Coiled-coil Protein Kinase
<b>ROCKi</b>	Rho-associated Coiled-coil Protein Kinase Inhibitor
<b>RPECs</b>	Retinal Pigmented Epithelial Cells
<b>rpm</b>	Revolutions per Minute
<b>SOX</b>	Sex Determining Region Y-box
<b>SUMO</b>	Small Ubiquitin-related Modifier
<b>TBS</b>	Tris-buffered Saline
<b>TGF</b>	Transforming Growth Factor
<b>WCB</b>	Working Cell Bank

# 1. INTRODUCTION

## 1.1. Human Pluripotent Stem Cells

Human stem cells are unspecialized cells which have unlimited potential for self-renewal and the capacity to differentiate into any cell from one of the three primary germ layers. Depending on the type of stimulus, they are able to deviate into the precursors of these cells, which would later give rise to fully differentiated cells, with a defined structure and function, that make up for the entire tissues and organs of the human body.

These cells can be found in particular parts of the human body such as in the umbilical cord blood, bone marrow, intestinal epithelium or adipose tissue. Stem cells can essentially be classified according to their differentiation potential: totipotent, which give rise to all embryonic and adult lineages; pluripotent, if they originate all cells types that compose an adult body; multipotent, if they are able to originate cells from multiple cells within one lineage, and finally unipotent, which mature into one type of cells<sup>1,2</sup>.

Due to the characteristics of these cells, an extensive investigation is on-going regarding the fields of gene therapy, regenerative medicine, drug screening and all sort of cell-based therapies. Even so, there are still a set of challenges to overcome, regarding ethical issues attached to the experiments and material used, the transition from the laboratory scale to the industrial scale, or the standardization of the processes.

Mesenchymal stem cells are multipotent stromal cells that are currently used in several clinical applications in the past years<sup>3</sup>. The main reason for the success of these cells is the easiness of collecting and maintaining them, needing only a short period of time before the establishment of the culture and the application of the cells. With these advantages, pluripotent stem cells have been taking into consideration a lot more since they promote a wider variety of options in future treatments, and their pre-differentiation state *in vitro* can guarantee a safe utilization<sup>2</sup>.

The human embryo naturally develops giving rise to all of the cells that composed a full human body. As previously commented, pluripotent stem cells can originate all cells from the three-primary germ layers, namely endoderm, mesoderm, and ectoderm. The endoderm (internal layer) gives rise to organs such as the lungs, thyroid and pancreas; the mesoderm (middle layer) becomes the cardiac muscle, skeletal muscle, smooth muscles, the tubule cells of the kidneys and red blood cells, and, finally, the ectoderm (external layer) develops into cells of the skin, melanocytes and the neurons of the brain<sup>4,5</sup>.

Since it has been investigating ways to treat, understand and overcome problems related to all of these layers previously named, pluripotent stem cells (PSCs) have been having a great focus. Essentially, the PSCs that are currently being used are human embryonic stem cells (hESCs) and human induced pluripotent stem cells (hiPSCs), both presenting already known advantages and disadvantages for their use.



### 1.1.1 Human Embryonic Stem Cells

The first time it was reported the culturing of mouse embryos in the uterus and derivation of embryonic stem cells (ESCs) from these embryos, done by Dr. Evans *et al.*, it was dated back to 1981<sup>6</sup>. In the same year, Dr. Martin proved to be possible to culture these embryos *in vitro* and differentiate them, opening a door to begin the laboratory research towards the study using these cells<sup>7</sup>. Later, in 1998, it was when Thomson and collaborators showed that it was possible to isolate and grow embryonic stem cells from the human species in a cell culture<sup>4</sup>. They used cells from human blastocysts which showed to have the capacity of self-renewal and staying undifferentiated when maintained *in vitro*, even after 4 to 5 months, before being turned into trophoblasts and derivatives from all three-primary germ layers<sup>4</sup> (Figure 1). These human embryonic stem cells can be obtained by fertilizing eggs from donors *in vitro* purposely for research use, most specifically in order to collect the inner cell mass of the blastocysts<sup>4,8</sup>.

Despite their renewal capacity and high potential for different applications being unquestionable, these cells still have issues attached to them. One of them is the fact that these cells might lead to the generation of teratomas when transplanted into a living host, especially depending on which tissue they are introduced into<sup>9,10</sup>. Another polemic issue has to do with the fact that the manipulation and destruction of viable human embryos have always been seen as a subject of controversy due to ethical and religious purposes<sup>11</sup>.

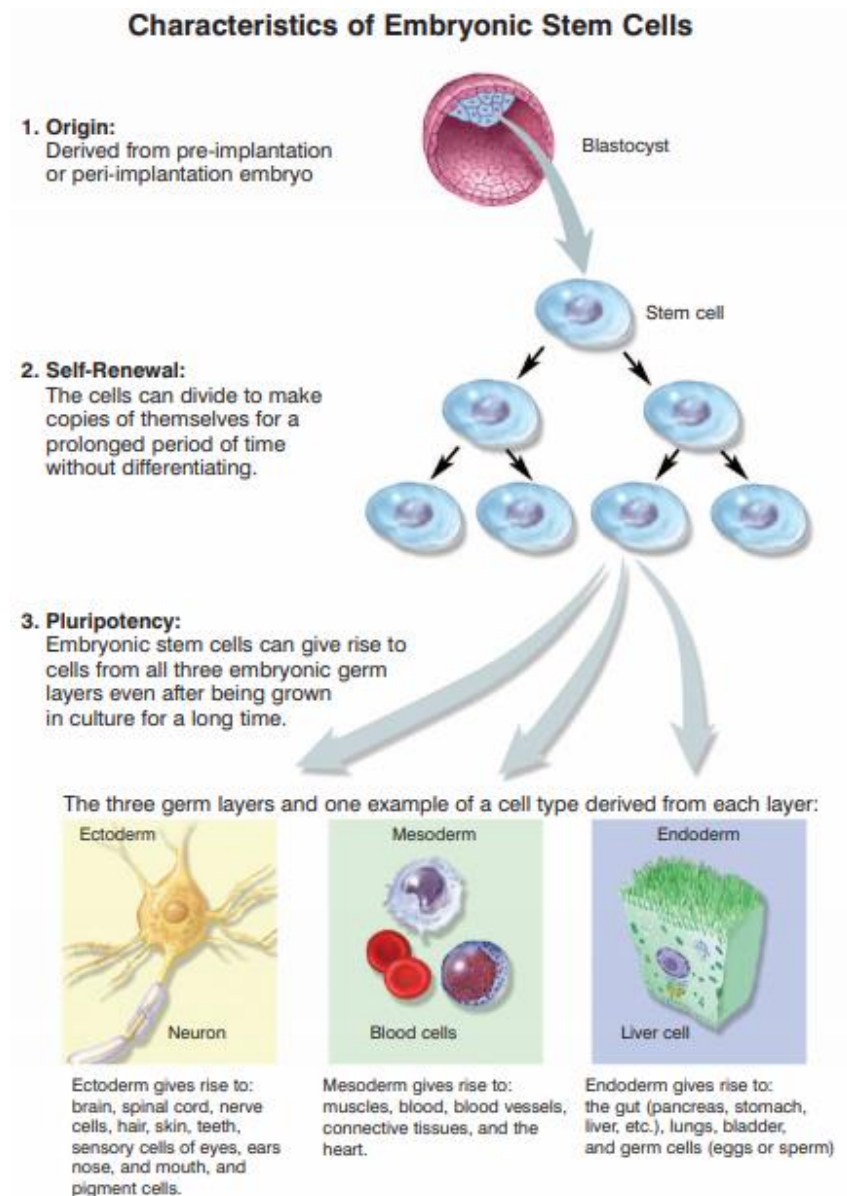


**Figure 1 - Characteristics of embryonic stem cells.** (Adapted from Winslow, T. in *Regenerative Medicine*, 2006)<sup>5</sup>.

### 1.1.2. Human Induced Pluripotent Stem Cells

Human induced pluripotent stem cells (hiPSCs) were first created in 2006 by Shinya Yamanaka and his collaborators by retrovirally, introducing specific genes encoding four transcription factors (Oct3/4, Sox2, Klf4 and c-Myc) into mouse embryonic fibroblasts, giving rise to a new generation of cells<sup>12</sup>. These cells have proved to be similar to hESCs, regarding their transcription program and chromatin modification profiles<sup>13</sup>, as well as in morphology, surface markers, overall gene expression and age-affected cellular systems, like telomeres and mitochondria<sup>14</sup>. One year later, it was possible to obtain hiPSCs by reprogramming adult dermal fibroblasts, targeting the same four factors, which implied

a step forward towards their research in humans<sup>15</sup>. These cells can be derived, not only from skin fibroblasts (Figure 2), but also from keratinocytes<sup>16</sup> and blood progenitor cells<sup>17</sup>.

The hype over these anchorage-dependent cells came mostly due to the way they could overcome major problems that other cells could not achieve as easily. The first one being the fact that the immune rejection after transplantation into the patient is much less probable when compared to the use of hESCs, since the cells are derived entirely from the patient<sup>5,18,19</sup>. The other one is that these cells were able to overcome some issues comparing to the utilization of human embryos, which carry more serious religious and ethical beliefs<sup>5,18,20</sup>. Also, these cells have an unlimited resource capacity since they can be obtained by performing a tissue biopsy, which anyone can easily donate, against the restricted supply capacity of hESC, derived from embryos discarded after *in vitro* fertilization. This also implies a much safer and less invasive alternative for users than eggs donation<sup>19</sup>.

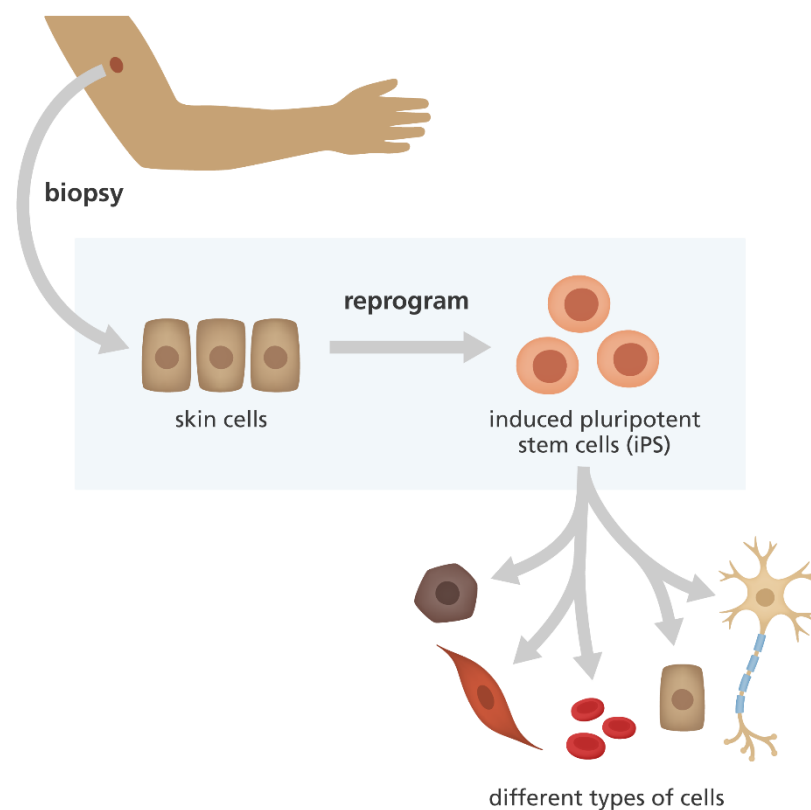


**Figure 2 - Skin cells can be reprogrammed into iPS cells that can then develop into different types of cells.** (Credit to Sanger Institute, Genome Research Limited, removed from <https://www.sanger.ac.uk/news/view/scientists-unveil-uk-s-largest-resource-human-stem-cells-healthy-donors>, accessed on 01/10/2018).

Even with all the advantages regarding these cells, there are still some issues that should be taken into account. The fact that it is being used viruses to induce said mutations, and even the cells themselves, which are genetically modified cells, might increase the risk of cancer by triggering

oncogenes or other cancer-causing genes<sup>18,21</sup>. Another factor that might lead to future implications, has to do with the age of the donor. Even though elderly patients are more plausible to receive treatment using these cells, the older the somatic cells are, the more likely of being mutated they are, due to the age and the long-term exposure to the external factors throughout their lives that can affect the quality of the cells<sup>22</sup>.

## 1.2. Applications of Human Pluripotent Stem Cells

Even with the previously named problems involving these cells, it is undisputable the potential attached to the research using them.

As referred before, stem cells are capable of self-renewal and differentiation, therefore they can be applied to a wide variety of fields, such as for cell-based therapy, drug screening, disease modelling and tissue engineering (Figure 3 and Table 1).

Cell-based therapies are processed by injecting into the host stem cells which, under certain conditions, will contribute to the reestablishment of function and integrity of the tissue they are inserted into. For example, studies regarding treatment for type I diabetes had been reported<sup>23</sup> in which the authors claimed to have generated functional pancreatic progenitors, from hESCs fair for clinical trials, with  $\beta$  Islet cells containing a subcutaneous capsule that present cell-mediated autoimmunity. Moreover, even if not yet in clinical trials phase, it was already possible to obtain mature  $\beta$  Islet cells *in vitro*<sup>24</sup>.

Furthermore, preliminary results have been already reported regarding retinal pigmented epithelial cells (RPECs) derived from hESCs for atrophic age-related macular degeneration and Stargardt's macular dystrophy<sup>25</sup>. Also regarding RPECs, the transplantation of a sheet of iPSC-derived RPECs into a Japanese patient was already performed without serious repercussions<sup>26</sup>. This could be an example of tissue engineering, which can be divided into three approaches: the use of bioactive molecules, such as growth factors, that contribute for tissues induction; the use of cells that respond to various signals and stimuli, and the construction of three-dimensional tissue-like matrixes capable of replacing damaged tissues or organs<sup>27</sup>. Therefore, the so-called regenerative medicine comprises both cell therapy and tissue engineering.

Additionally, stem cells can be also used for drug screening and disease modelling. This means that the pharmaceutical industry takes advantage of these cells to develop new medicines and innovative treatments. In a paper published in 2017, it was created functional downsized gut organoids from both hESC and iPSC, using a xenogeneic-free medium, suitable for drug screening and the study of several intestine diseases<sup>28</sup>. As for another study done in 2016, the scientists were able to concretize an allogeneic transplantation of iPS cell-derived cardiomyocytes into primate hearts, successfully ensuring the graft survival for at least 12 weeks<sup>29</sup>. Human embryonic stem cell-derived oligodendrocytes have also been used and proved to regenerate myelination and behavioural deficiency of irradiated rats<sup>30</sup>.

Moreover, this also means that the pharmaceutical companies can use these cells for a development of a tailored treatment, such as acquiring the patient disease-affected cells and converting them into iPSCs before differentiating them back into somatic cells. This allows, not only to understand the mechanisms involved in the development of the phenotype typical of the disease, but also to test the toxicology and different drugs for its efficient treatment, without directly affecting the patient<sup>31</sup>. Also, since the cells are harvested directly from the patient, this also means an increase in terms of safety towards immunogenic response<sup>32</sup>.

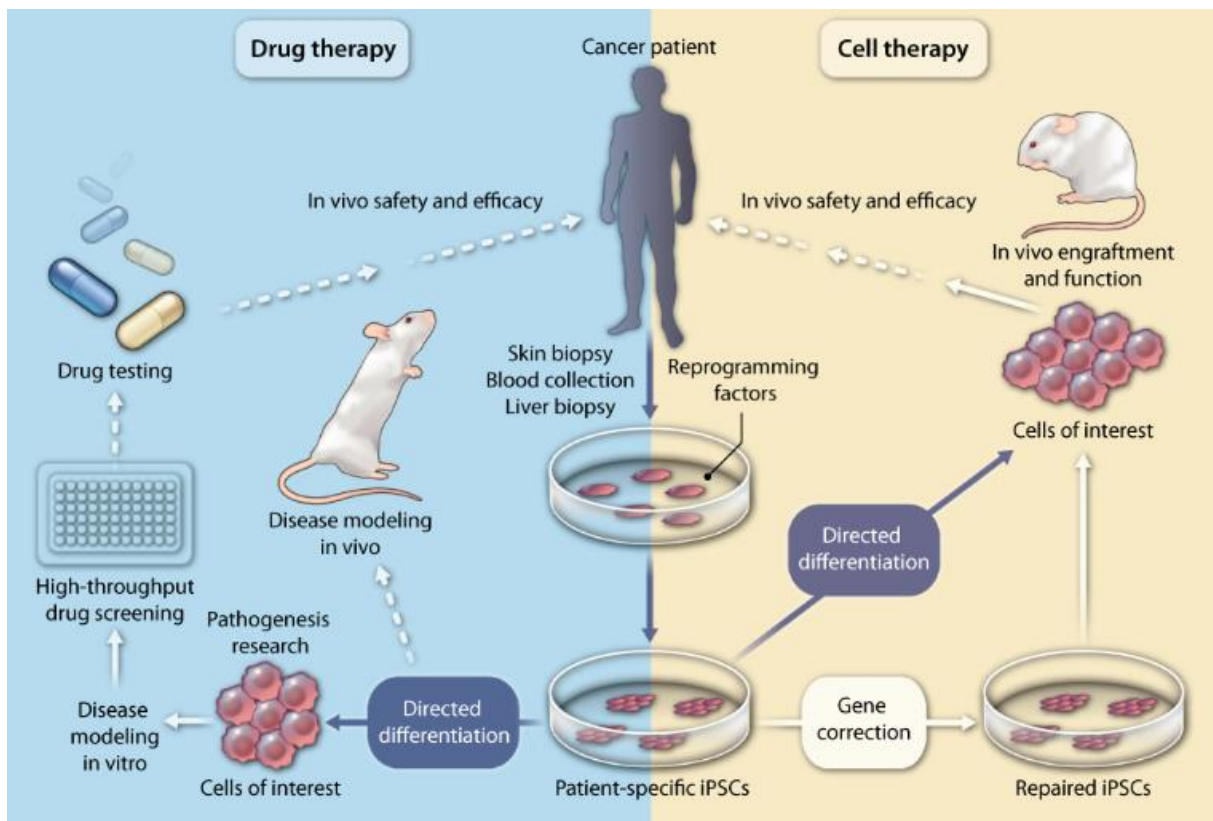


**Figure 3 – Roadblocks to translating human iPSC technology to the clinic.** Human iPSCs technology potentially can be used for screening new cancer drugs (blue box) and ultimately for providing cells for transplant to treat a variety of diseases, including cancer (yellow box). Genetic mutations can be corrected in patient-derived iPSCs by gene targeting approaches. The main hurdles to using patient-specific iPSCs for disease modelling, drug screening, and transplantation purposes are **(i)** a lack of effective differentiation protocols, **(ii)** little or no engraftment capability for the majority of human iPSC-derived specialized cells, **(iii)** difficulties in modelling multifactorial diseases, **(iv)** the need for GMP-compliant conditions at each step, and **(v)** safety concerns regarding the potential tumorigenicity of iPSCs associated with their pluripotent state or with insertional or culture-driven mutagenesis. Dotted arrow not yet tested; solid arrow, only a few studies available; blue arrow, feasible but requires further study. (Adapted from Sharkis *et al.*<sup>33</sup>, National Institute of Health Public Access).

**Table 1 - Examples of clinical trials using human embryonic stem cells (hESCs) and induced pluripotent stem cells (iPSCs).** Clinical trials as from 2016. RPE – retinal pigment epithelium (adapted from Trounson A. *et al.*<sup>34</sup>).

<b>Trial Sponsor (Location)</b>	<b>Disease Target</b>	<b>Cell Therapy</b>	<b>No. Patients</b>	<b>Phase</b>
Chabiotech Co. Ltd. (S. Korea)	Macular Degeneration	Human-ESC- derived RPE	12	Phase I/II
Ocata Therapeutics (MA, USA)	Stargardt's Macular Dystrophy	Human-ESC- derived RPE	16	Phase I/II
	Macular Degeneration	Human-ESC- derived RPE	16	Phase I/II
	Myopic Macular Degeneration	Human-ESC- derived RPE	Unknown	Phase I/II
Pfizer (UK)	Macular Degeneration	Human-ESC- derived RPE	10	Phase I
Cell Cure Neurosciences Ltd. (Israel)	Macular Degeneration	Human-ESC- derived RPE	15	Phase I/II
ViaCyte (CA, USA)	Type I Diabetes mellitus	Human-ESC- derived Pancreatic Endoderm Cell	40	Phase I/II
Assistance Publique-Hopitaux de Paris (France)	Heart Failure	Human-ESC- derived CD15+ Isl- 1+ Progenitors	6	Phase I
International Stem Cell Corp. (Australia)	Parkinson's Disease	Human Parthenogenic- derived Neural Stem Cells	Unknown	Phase I/II
Asterias Biotherapeutics (CA, USA)	Spinal Cord Injury	Human-ESC- derived Oligodendrocyte Precursor Cells	13	Phase I/II

## 1.3. Expansion of Human Pluripotent Stem Cells

Transiting from the laboratory experiments to an industrial scale is still a challenge, not only because of the initial small working number of cells, but also because the success of the process also depends on the perfect equilibrium between the optimization of the culture parameters and the design of the culture vessel, while maintaining Good Manufacturing Practices (GMP) at all times.

Especially in the cases of both hESCs and iPSCs, these are obtained in small quantities, which in most cases compromises their use in later therapeutic applications. A low number of these cells have already progressed into clinical stages, but the goal of treating large numbers of patients requires a cell cultivation system at a larger scale<sup>34</sup>.

### 1.3.1. Xeno-free, Feeder-free and Chemically Defined Culture Systems

One of the main concerns in the culturing of stem cells is the stability of the conditions the cells are cultured in. The worry is not only to find an ideal protocol for the production and later safe and secure application of stem cells into regenerative medicine or drug screening, but also perform it while maintaining good manufacturing practices (GMP). GMP, as defined by regulations from both the European Medicines Agency<sup>35</sup> and the Food and Drug Administration<sup>36</sup>, is composed by a set of factors that promote the execution of experiments that are free from contaminants and that use animal-free culture medias, feeder-free cells or feeder-free matrix for every step of the production of these cells, either it is derivation, passaging or even cryopreservation<sup>37</sup>. It also moves towards the standardization of the process of culturing the cells, leading to insignificant or even none batch-to-batch variability in the future.

As previously said, the use of a xeno-free medium is a way to minimize the risk of growing cells using other animal-derived substances which are essential for their growth. The use of defined components from the same origin as the cells that are under study would contribute to a more confident practice for future therapeutic applications. For example, fetal bovine serum (FBS), rich in growth factors and other components for *in vitro* cell culturing, is being replaced whenever a better alternative is available<sup>38</sup>.

Furthermore, it is also common to use feeder cells to maintain the undifferentiated state of stem cells. These frequently are fibroblasts, which produce indispensable substances, such as growth factors, proteins and extracellular matrix (ECM) components<sup>39</sup>. Feeder-cells, such as mouse embryonic fibroblasts (MEF), have been used before<sup>39-41</sup>, but the constant concern for xeno-free conditions has brought to light the use of human feeder cells, like human fibroblasts<sup>41-43</sup>, to closely reproduce the *in vivo* conditions towards clinical testing in humans. However, more and more the process is trying to be simplified, meaning that the use of feeder-free culture is being encouraged<sup>38,41,44,45</sup>.

Chemically defined culture systems allow the increase of the reproducibility of the results, which consequently will lead to a more consistent batch-to-batch result, contrarily to the use of feeder cells or FBS<sup>46</sup>. For example, a chemically developed defined medium named TeSR1 (a defined culture medium containing FGF-2 (fibroblast growth factor-2), lithium chloride (LiCl), g-aminobutyric acid (GABA), TGF- $\beta$  (transforming growth factor- $\beta$ ), and pipercolic acid) was shown to be useful in the derivation of two new hESC lines in a chemically-defined culture<sup>47</sup>. Another medium, the E8 medium, which is a derivate of TeSR1 containing eight components that lacks  $\beta$ -mercaptoethanol, is believed to be suitable for different lines of hESCs and hiPSCs<sup>48,49</sup>.

All in all, an effort is being made to promote the development of this technology using xeno-free conditions, feeder-free culture systems and chemically defined formulas to target the full standardization of the processes and guarantee their safety for therapeutic purposes. The challenges for growth conditions include the determination of the long-term effects of the several conducts and their differentiated origins, the need to vehemently verify the preclinical safety of the final products, either *in vitro* or *ex vivo*, and how the products must show anticipated safety and desired functionality before being applied into the patients<sup>46</sup>.

### 1.3.2. Process Standardization

The ultimate goal for the application of stem cells in regenerative medicine and other fields is to guarantee a final and standard protocol for the production of the cells, which are obtained according to the case they will be used for. Treatments using, for example, mesenchymal stem cells, which are multipotent stromal cells, are already being used since they have very little or no repercussions to the patients<sup>50</sup>.

Nowadays, cell banks are places in which certain types of cells are replicated, frozen and stored for later use for research and medical purposes, after being well studied and stable. Certain groups that are already suitable for product development, either for therapeutic use or for commercialization, are part of what is called a master cell bank (MCB). The later stages of their development, corresponding of cells that will undergo a process of scaling-up for future applications after being selected, grown in a culture and passaged several times before being cryopreserved, are part of a working cell bank (WCB)<sup>51</sup>.

Cell banks are supposed to be flexible and adaptable to the constant needs, while using the currently available methods and while maintaining the quality and safety that has to be guaranteed to both the patients and the sponsors. These banks must also be resourceful, meaning that the material used has to be economical and practical to be sustainable and meet the community's needs. Finally, they have to correspond to the ethical standards and guidelines of the country they are inserted into<sup>52</sup>.



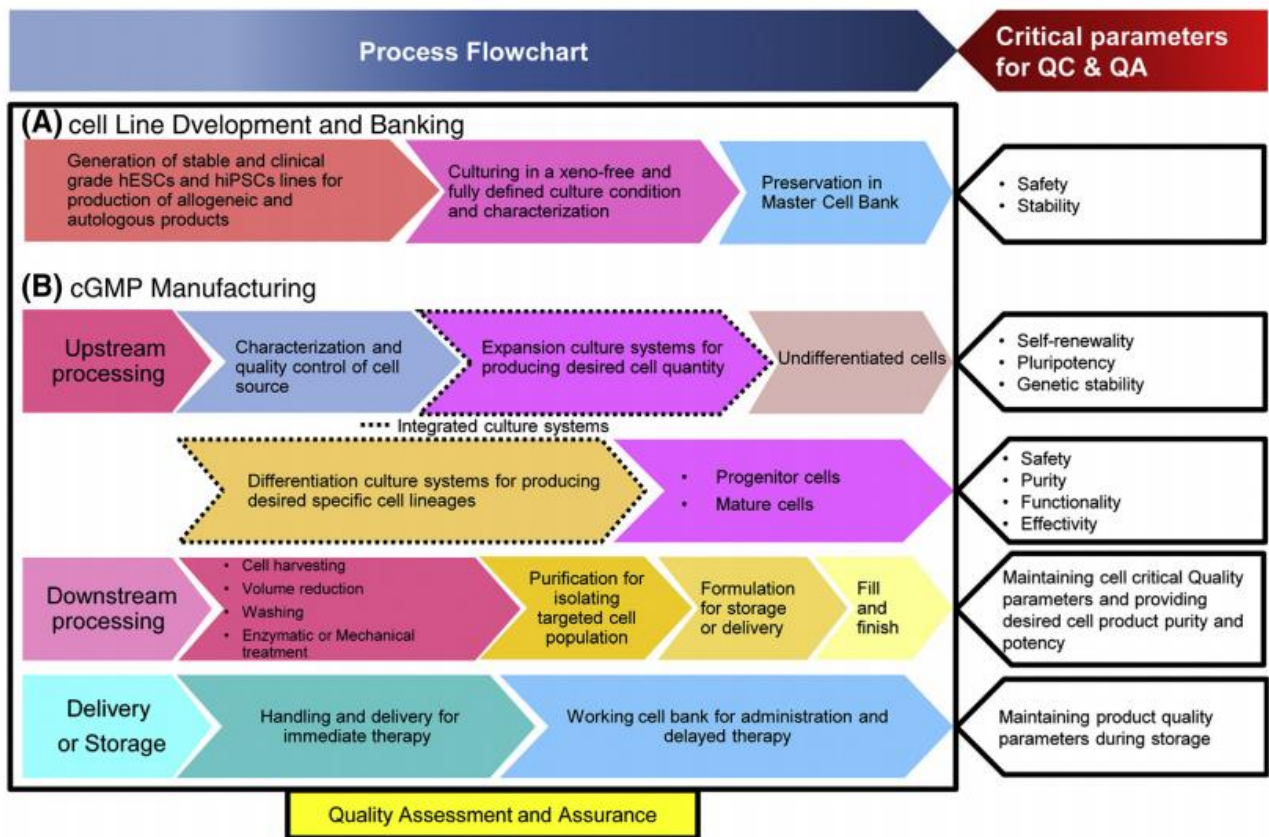


**Figure 4 – Process flowchart for cGMP manufacturing of hPSC-based therapeutic products and critical quality parameters related to each step of processing.** The process flowchart is divided into **(A)** cell line development and banking and **(B)** cGMP manufacturing sections. In the cell line development and banking section, clinical grade hPSCs are produced using safe derivation or reprogramming technologies, which have been characterized after their maintenance in xeno-free and fully defined conditions before cryopreservation in master cell banks to be used as the main starting material for cGMP manufacturing. The cGMP manufacturing process is divided into three main processing stages including upstream processing, downstream processing, and delivery or storage. In upstream processing, hPSCs are expanded and differentiated to targeted cell therapeutic products. The targeted cell products are isolated and purified, formulated and/or filled for instant or delayed delivery. In the delivery or storage stage, the therapeutic cell products are handled and transferred to the final user or patient or preserved in large working cell banks for delayed delivery. A robust quality control (QC) and quality assurance (QA) system will control and monitor the whole manufacturing process based on critical quality parameters in each processing step. (Adapted from Abbasalizadeh *et al.*<sup>53</sup>).

The age of the donor and the source of the cells for these banks influence their regenerative capacity. Genomic and epigenetic modifications are prone to happen in aging cells, which largely contributes to differences in the cellular pathways. This year, it was studied the global chromatin structure in human adipose-derived stem cells (ASCs) and compared it to the chromatin structure in age-matched fibroblasts via ATAC—seq technology. Aging ACSs showed to globally have more stable chromatin accessibility profiles when comparing to aging fibroblasts, meaning that robust regulatory

mechanisms are more efficient on the maintenance of the adult stem cell chromatin against ageing than in differentiated cells like fibroblasts. Also, age-dependent cells had subtle changes in the nucleosome position, together with the expression of a small ubiquitin-related modifier (SUMO), a protein that regulates the cellular pathways under stress conditions such as heat-shock, contrarily to old fibroblasts<sup>54</sup>.

However, and as commented before, slight changes in the handling of the cells might be sufficient to lead to different and unexpected results, meaning that the overall operator skill is also a point to be considered. Long-term stability of the undifferentiated state of PSCs is complicated regarding technical level of robotics and automation. Even though, it had been reported before that a fully automated culture system that automates cell seeding, medium changing, cell imaging and cell harvesting was able to culture iPSCs on feeder cells for 60 days and 20 passages, while maintaining their pluripotency and capacity of differentiation in specific types like dopaminergic neurons and pancreatic islet cells<sup>55</sup>.

The passaging of the cells is also one issue to be taken into account. Even if the handling of the cells does not bring any kind of damage to the culture in the end, batch-to-batch variability might still happen when using enzymatic dissociation, due to the decreasing activity of the enzymes and their quality. The use of chemically defined systems for the detachment of the cells would be a solution to attenuate this problem<sup>56</sup>.

Furthermore, even the same cell type, but different cell lines, for example, for hiPSCs cell lines Tic and 253G1, might lead to significant differences in growth kinetics and morphology depending on the type of environment they are cultured in and, thus, it is of interest to understand which would be the best methodology for their maintenance and growth<sup>57</sup>.

The characterization of the ESCs and iPSCs and their different lines is essential to understand how variations on their characteristics might influence their utility and safety for clinical applications. Such differences were studied before for 20 lines of previously derived ESCs lines and of 12 hiPSCs lines in order to draw genome-wide reference maps of DNA methylation and gene expression<sup>58</sup>. With this, it would further help to understand the epigenetic and transcriptional similarities in these lines and assess the differentiation potential in each case.

### **1.3.3. Passaging of Human Pluripotent Stem Cells**

These cells are support-dependent cells, meaning that they need a surface to attach to in order to proliferate. Therefore, one technique used for the expansion of hPSCs is sub-culturing them into a new culture system with fresh medium and components that allow them to proliferate. The process of individualization of the cells before transferring them into a new culture system is named cell passaging.

The most common way to effectuate the passaging step is by using enzymatic methods, which promote the dissociation of the cells to the surface and to one another, encouraging their individualization for later seeding into the new system. The fact that these cells are very sensitive to

sudden changes of environment they were previously settled in and to the way they are handled, can result in cell death during the procedure. However, there are certain substances, such as the Rho-associated protein kinase (ROCK) inhibitor that can be used in order to reduce cell apoptosis and, thus, increase their survival rate<sup>59</sup>.

### **1.3.3.1. EDTA and Trypsin in Cell Passaging**

One classic technique used for the expansion of hPSCs is sub-culturing them into a new culture by using ethylenediaminetetraacetic acid (EDTA) and trypsin.

EDTA is a general chelator of  $\text{Ca}^{2+}$  and  $\text{Mg}^{2+}$ , two divalent cations that exist on the surface of the cells. When it binds to the receptors on the surface of the cells, it will promote cell-cell and cell-extracellular matrix (ECM) dissociation by inhibiting integrin-ligand binding<sup>60</sup>.

Trypsin is a protease that acts by digesting amino acids from the ECM that participate in the adhesion of the cells, further promoting their individualization and detachment from the surface, and guarantee the entire removal of the cells from the dish.

This process is efficient, though it should be done quickly, before cells began seeking for support one to another, forming small-sized aggregates that might compromise counting. It is also essential to do the process as gently as possible, since the procedure is likely to cause a significant cell loss before seeding.

### **1.3.3.2. ROCK Inhibitor**

As commented before, the maintenance of the survival of the cells after detachment is a challenge, compromising the research. However, it was shown that the use of the ROCK inhibitor, Y-27632, controls cellular functions such as cell shape, motility, secretion, proliferation and gene expression<sup>61</sup>. For cells such as hESCs, it prevents dissociation-induced apoptosis, increases cloning success, and also facilitates sub-cloning after gene transfer<sup>59</sup>.

The ROCK protein is part of the family of serine/threonine-specific protein kinases, which is activated by the interaction with the small GTP-binding protein RhoA. This protein and ROCK are present in crucial physiological function in the contraction of smooth muscle, cell proliferation, adhesion, migration and inflammatory responses<sup>62</sup>. This kinase was found to mediate RhoA-induced actin cytoskeletal changes by the phosphorylation of myosin light chain<sup>63</sup>. This actin-myosin based cytoskeleton is vital for the contraction, motility and tissue organization of the cells. Actin-myosin motors are made of actin filaments and non-muscle myosin II heavy chains (MYH). The actin filaments are usually attached to integrins, through focal-adhesion, and E-cadherins, through  $\alpha/\beta$  catenin complexes. By hydrolysing ATP by the MYH ATPase, energy is generated which makes possible for the MYHs to slide along the actin filaments, provoking their contraction<sup>64</sup>. When cells are separated from the ECM and from one to another, the actin-myosin contracts, leading to differences in the phenotype, including

membrane blebbing, a sign of apoptosis<sup>65</sup>. If the contraction continues due to the lack of adhesion of the cells, then it will ultimately result in their death.

Therefore, the Y-27632 is used during passaging and even after seeding to prevent cell death and to enhance colony formation, since it inhibits the signalling pathway that triggers the contraction mechanism (Figure 5). This also includes the success it has in cases in which the exploration of the pluripotency state of the cells and the formation of the aggregates are involved<sup>59</sup>.

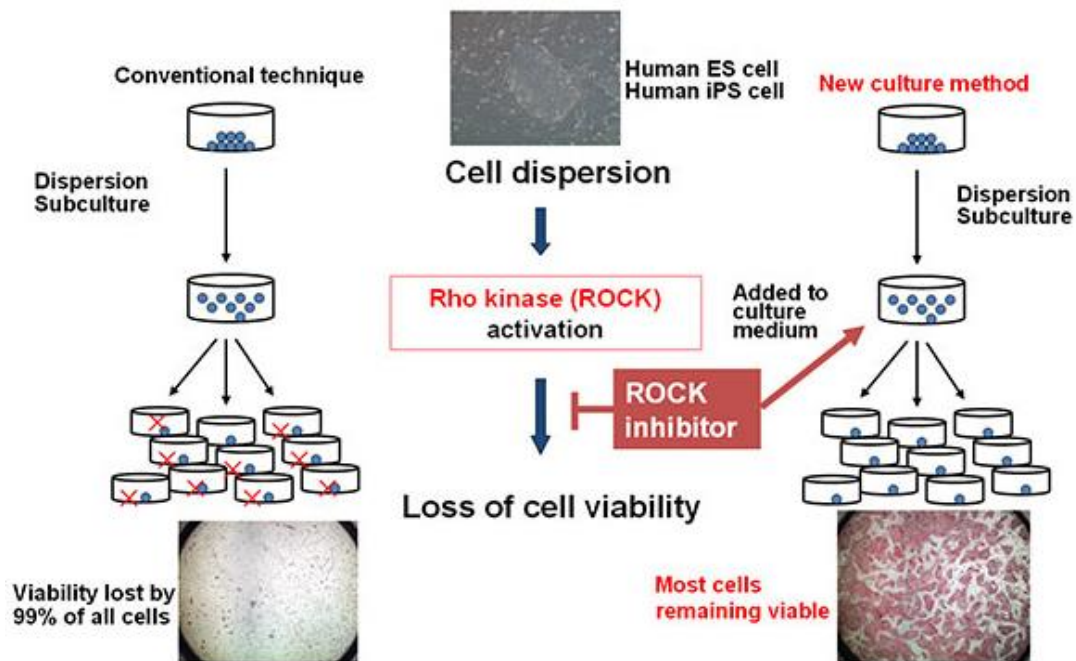


**Figure 5 – Discovery of the method for suppressing loss of dispersed human ES cell viability with the use of the ROCK inhibitor.** (Removed from [https://www.mst.or.jp/portals/0/prize/english/winners/bio/bio2012\\_en.html](https://www.mst.or.jp/portals/0/prize/english/winners/bio/bio2012_en.html), accessed on 18/09/2018, based on the works of Watanabe *et al.*<sup>59</sup> and Ohgushi *et al.*<sup>66</sup>).

### 1.3.4. Large-scale Expansion of Human Pluripotent Stem Cells

It is widely agreed that stem cells are one of the paths for the development of technology regarding modern medicine.

Some methodologies have already been implemented according to the cell source, the desired final product and its specifications, but the improvement of the culturing vessels is still a constant need. As emphasized before, the global aim for the large-scale production of hiPSCs targets their reproducibility, safety and clinically approved products. Having these in mind, it is of concern to evaluate some of the most important particularities. These could include the process of scaling up instead of

scaling out, meaning having a single culture in a larger volume, instead of distributing it through different smaller vessels, in order to maintain homogeneity and to avoid contaminations. The use of a dynamic culture that improves mass transfer, the circulation of oxygen and nutrients and the homogenous distribution of the cells in the culture, could also guarantee the consistency of the given final results. This can be currently done by rotating platforms, air-based mixing, impeller-based mixing and rocking. However, the shear force applied to the cells is one of the main factors to be considered before choosing a suitable mixing procedure, since it can damage them<sup>57</sup>. Moreover, continuous medium change is also crucial for the stability of the culture conditions, either for providing the cells the factors they need to proliferate or to remove their waste products. Little changes in the culture conditions, such as pH, temperature, oxygen concentration or growth factors could be sufficient to lead to unexpected results, such as unwanted differentiation or even cell death. Avoiding human error by promoting a more automatic monitoring and control of the process to ensure the supposed culture conditions in real time would definitely help the standardization of the process. And finally, it is also imperative to take into account the balance between the cost of the process and its efficiency and the yield of the final product<sup>67</sup>.

Therefore, scaling-up the production of stem cells for regenerative medicine is undoubtedly one of the greatest challenges in this field. So, it will be described the platforms and results for large-scale expansion of pluripotent stem cells, using microcarriers and in the form of 3D aggregates, in the different bioreactors currently available on the market. It will also be addressed an approach about the parameters that contribute to the optimization of the culture conditions.

#### **1.3.4.1. Platforms for Large-scale Expansion of hPSCs**

There are several platforms available on the market that can be used depending on the final goal and regarding their advantages and disadvantages (Figure 4).

These support-dependent cells are traditionally grown in monolayers colonies on an ECM or fibroblast feeder layers. Thus, T-flasks provide a 2D environment for cell proliferation and they are possible to be used for large-scale expansion, in particular if multiple vessels are used at the same time, in the same conditions (scaling-out). It is useful in cases that a small number of cells are required for the final product, for toxicity testing or if the tissue in study allows the use of this method. The growth of retinal pigment epithelium cell sheets from hiPSCs could serve as an example since the morphology and physiology characteristics of this tissue *in vivo* can be more easily reproduced in these conditions to mimic the reality<sup>68</sup>. The problems with T-flasks is that the medium cannot be continuously changed, real-time monitoring is not possible and, most importantly, expansion is only efficiently achieved if small-scaled<sup>67</sup>.

Among the current methods used, scaling-out using multiple vessels is a common practice, useful if the final product requires a small number of cells, existing some multi-layered 2D static vessels available in the market<sup>67</sup>. However, the static culture conditions bring limitations in terms of expansion because of its low yields, non-homogenous nature, demanding constant monitoring and control,

extensive handling procedures and absence of flow<sup>69</sup>. For instance, a patient needing a cardiomyocyte replacement would require up to  $4.00 \times 10^{10}$  cells to treat the condition, meaning it would be necessary up to 1144 T-175 flasks per patient, which would be an unbearable task<sup>70</sup>.

Thus, and as mentioned before, only by scaling-up it is possible the obtention of the necessary amount for certain applications, as well as a more cost-efficient process.

Spinner flasks offer one of the many solutions for the expansion of pluripotent stem cells, since they behave as a laboratory-sized stirred tank bioreactor. Since these vessels can be equipped with culture conditions controllers, it makes the process more standardized and with less batch-to-batch differences. When in suspension, cells attach to each other, forming aggregates which can be kept in these platforms with constant shaking, such as orbital shaking. Even with these advantages, transiting to bioreactors in order to work with larger volumes is still the major step in terms of scaling-up<sup>67</sup>.

Other solutions have already been implemented, such as rotary cell culture systems and cell culture bags. Rotary cell cultures, like the Synthecon<sup>®</sup>, or roller bottles, are rotating 3D vessels that permit a dynamic flow with the perk of, since the rotation promotes the agitation of the culture, creating an environment with low shear-stress. Even if some authors have commented on the positive results of these bioreactors<sup>71</sup>, their volume is limited to larger applications, and concentration gradients are minimized, albeit they still persist<sup>72</sup>.

As for cell culture bags (WAVE Bioreactor<sup>™</sup> or BIOSTAT STR<sup>®</sup>), the rocking intensity promotes the homogeneity of the medium and these bioreactors also enable a constant control of the culture conditions and the disposal of material at the end of the process (single-use bags). These were shown to be very efficient for the expansion of murine iPSC and their differentiation into cardiomyocytes under a hypoxic environment, in comparison with other existing protocols that needed expensive components for the medium and low yields were obtained for this aim<sup>73</sup>.

Some other existent bioreactors such as hollow-fiber bioreactor and fixed and fluidized bed bioreactor have shown to be good in the differentiation of hematopoietic stem cells and mesenchymal stem cells<sup>72</sup>. The first type has two-components systems composed of intra-capillary and extra-capillary spaces where the medium flows<sup>74</sup>. They increase the contact area between the cell culture and the medium, though it has complications regarding monitoring and scale-up as well. As for fixed and fluidized bed bioreactors, they are composed of a column that can be filled with particles, either packed ones (fixed bed) or floating ones (fluidized bed). Even if these platforms permit a 3D scaffolding for the culturing of these cells, spatial concentration gradients (in packed bed reactors) and shear stress effects (fluidized bed) is still a reality<sup>72</sup>. Therefore, the focus has been moving towards the exploration of the potentialities of stirred-tank bioreactors.

At the moment, stirred-tank bioreactors are the most motivational platform for the scale-up of hPSCs. They have problems of scale-down in case of studying high-throughput applications, and the hydrodynamic shear-stress is also something that should be taken into account. Even though, with these, it is possible to promote a fully equipped system for real-time control of temperature, oxygen partial pressure, pH, among other parameters. They also permit to equip the impeller needed for the

agitation towards a homogeneous and dynamic stirred medium in order to obtain enough quantity of cells for future clinical applications, since they permit the increase of the working volume (up to 200 L)<sup>75</sup>.

As a consequence of the constant improvement of the performance of these bioreactors (Figure 6), the microcarrier-based dynamic suspension cultures and aggregate-based 3D suspension cultures were introduced and they are currently the favourable ones for large-scale production of human pluripotent stem cells, mainly hESC and iPSC.

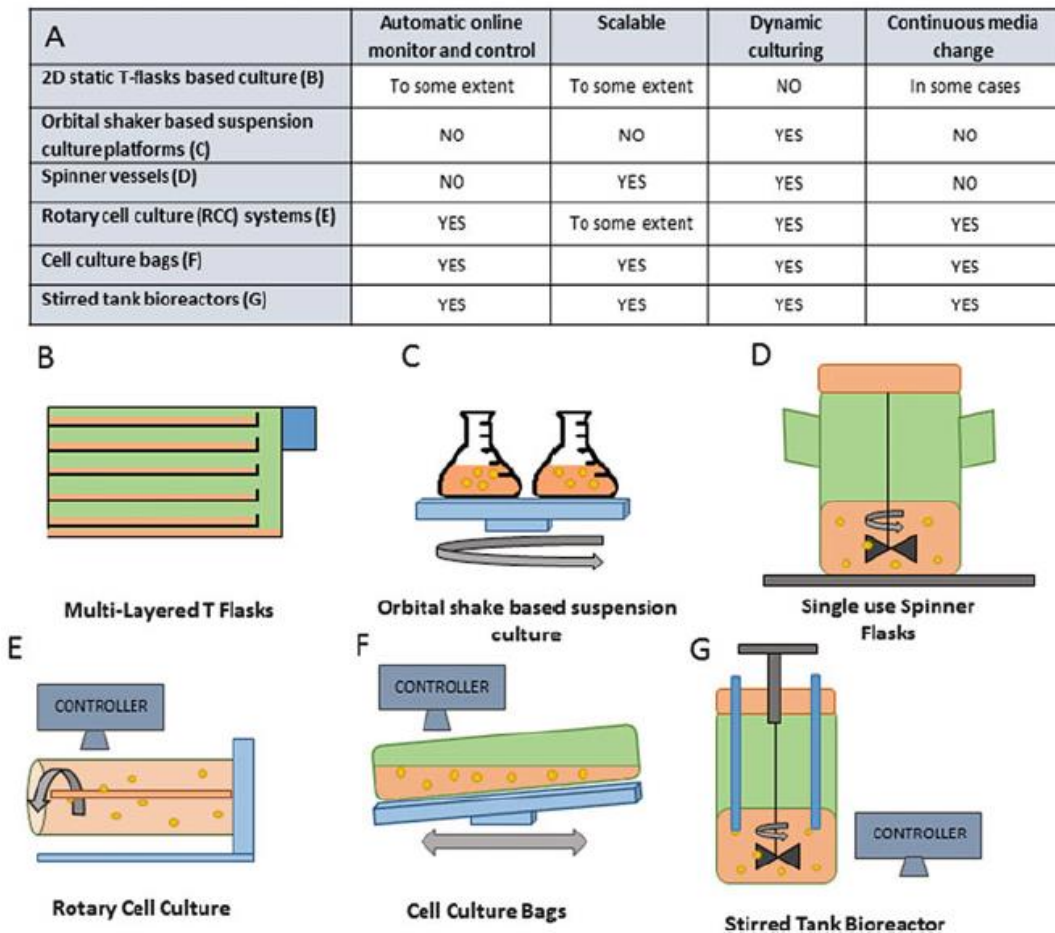


**Figure 6 - Platforms for large-scale expansion of hPSCs.** (A) Comparison of the various platforms and their properties; (B) 2D static T-flask-based cultures are scaled out, adding more layers and enlarging the culturing surface. In the Xpansion® (ATMI) system, continuous media change and online monitoring are available; (C) 3D-aggregate culturing on orbital shakers is suitable for process development and small-scale protocol optimization; (D) Spinner flasks can act as a preliminary step before moving to a stirred-tank bioreactor because the agitation techniques are similar. However, the system is not monitored and does not allow continuous media change; (E) Rotary cell culture system is suitable for small-scale optimization of hPSC expansion and differentiation; (F) Cell culture bags are applicable for GMP manufacturing. They are single-use and equipped with online sensors and a perfusion system; (G) Stirred-tank bioreactors are widely used and easily scaled up. They are extremely flexible and suitable for multiple applications, enabling continuous media change and online control and monitoring of culture parameters. (Adapted from Lavon *et al.*<sup>67</sup>).

### 1.3.4.2. Microcarrier-based 3D Dynamic Suspension Cultures

The need to overcome the barriers the 2D static cultures impose brought to light new advances, in which it was inserted the microcarrier technology.

The microcarriers are microparticles that provide a matrix and support for these anchorage-dependent cells that, together with a suspension culture, lead to a higher surface area in contact with the medium and, thus, an increase of the productivity<sup>76</sup>. Additionally, along with a controlled system and the right level of agitation, the process can be enhanced<sup>70</sup>. For instance, in 2016, 25 rpm was shown to be the ideal agitation rate for the expansion of iPSC in a spinner flask, while using microcarriers<sup>77,78</sup>.

Typically, the microcarriers suspension are kept in spinner flasks, which, as said before, are regarded as bioreactors at a laboratory scale, though once the passage to stirred-tank bioreactors for industrialization becomes a fully standardized practise, it is expected to have even higher yields<sup>76,79</sup>.

Choosing the right characteristics of the microcarrier also contributes to the final result (Figure 7). These could be microporous (pore diameter smaller than 1  $\mu\text{m}$ , allowing the cells to adhere and growth on the external surface of the support), macroporous (pore diameter usually between 10 and 50  $\mu\text{m}$ , allowing the cells to adhere and growth on the internal surface of the support) or nonporous (like Cytodex 1 and Cytodex 3)<sup>79</sup>. For example, it had been tested before ten types of microcarriers on hESC in terms of attachment efficiency, growth and pluripotency<sup>80</sup>. It was concluded that Matrigel<sup>TM</sup>-coated or laminin coated microcarriers showed to be better for the maintenance of pluripotent cells for longer periods of time and successfully expand them in spinner cultures. As for other supports tested, such as macroporous beads and small diameter (65 and 10  $\mu\text{m}$ ) spherical microcarriers, the results found were not so motivating, since these beads provided a non-uniform exposure of cells to the medium compounds.

Moreover, not only the support itself makes a difference, but so does the surface coatings in certain cases. These cells need a defined extracellular matrix, such as Matrigel<sup>TM</sup>, containing proteins, like fibronectin, for the expansion and later differentiation of the cells<sup>76,78,81</sup>. Yet, the use of these substrates limits the applicability for later therapeutics purposes that need good manufacturing practises, meaning that the use of xenogeneic-free materials as surface coatings is still a preferable solution once fully adapted<sup>82</sup>. It had been conducted an experiment using microcarriers and a serum-free medium for the scale-up in a stirred-tank bioreactor of mouse embryonic stem cells, in which it was obtained an  $(85 \pm 15)$ -fold increase in 11 days and the expression of makers proved that the pluripotency of the cells was maintained<sup>83</sup>.

Initially, these experiments were mostly performed using hESC, but after the iPSC turnover, and due to the resemblance in terms of morphological characteristics to each other, some studies have been using these too. Apart from that, the use of xeno-free conditions is still a motivation to explore new methodologies. Some recent studies have been capable of achieving these conditions to a certain extent. Previously, back in 2013, hPSC were tried to be differentiated into mesoderm progenitors in spinner flasks with success<sup>84</sup>. It was engineered polystyrene microcarriers with a vitronectin-derived



peptide surface for the attachment of the cells. With the specific care, it was possible to obtain an efficiency up to 40% and an average of a 24-fold increase in concentration per 6-day passage, with a viability over 85%. Moreover, in the following year, iPSC were also expanded in spinner flasks under chemically defined conditions, using a single-cell strategy for the inoculation of the cells in order to guarantee a more homogenous distribution throughout the microcarriers, after selecting the most suitable ones under static conditions<sup>85</sup>.

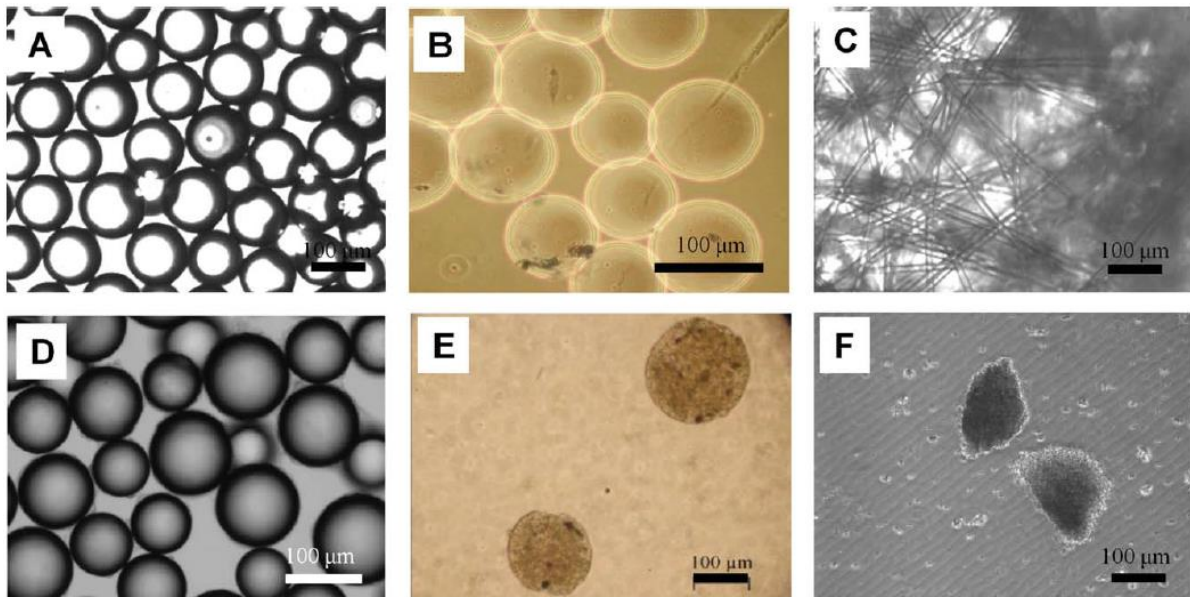


**Figure 7 - Morphology of various types of microcarriers (MCs).** (A) Glass (SoloHill) MCs as spherical beads; (B) Cytodex-3 as spherical beads; (C) Fibra-Cel<sup>®</sup> with porous microfibers; (D) Synthemax<sup>®</sup> II MCs with vitronectin peptide acrylate surface; (E) rat cartilage MSCs grown on CultiSpher-S; (F) PSC-derived extracellular matrix MCs. (Scale bars = 100 µm, adapted from Sart *et al.*<sup>86</sup>).

More recently, in 2016, different solutions were tested. It was the first time the Essential 8<sup>™</sup> xeno-free medium and xeno-free vitronectin matrix for the expansion of human iPSC in stirred microcarrier culture systems was tested. The maintenance of the pluripotency of the cells during expansion and induction of differentiation later into cells from neural and cardiac lineages was accomplished<sup>87</sup>. In another example it was used layer-by-layer designed microcarriers for iPSC, allowing a greater mass transport from the medium to the cells, while keeping a protected environment for them to proliferate. It was also made the comparison between these carriers as a delivery tool for iPSC to viral particles and liposomes, concluding that the size and surface charge of the cell colonies used influenced the layer-to-layer microcarrier uptake<sup>88</sup>.

Even if this method is better than static cultures, some problems have been pointed out as well. One of them is the fact that the microcarrier cultures are not homogenous, in other words: the cells are not spread over the surface evenly and the microparticles tend to adhere one to another after a while in

suspension<sup>67</sup>. As a result, the mass transfer of oxygen, growth factors, nutrients, among others, between the cells and the medium will differ, and unwanted differentiation might happen, diverging the results from what it is intended. However, even if none of these limitations are an issue, there is still a problem of detaching the cells, especially hESC, when comparing with, for example, murine embryonic stem cells<sup>89</sup>, from the microcarriers at the end of the process, or at least trying to integrate the microcarriers plus the attached cells as a whole into the final product. In certain cases, the culture maintenance and the harvesting complications make questionable the commercial viability of the cells<sup>67</sup>.

### 1.3.4.3. Aggregate-based 3D Cultures

In the turn of the millennium, it was realized that hPSC, when present in an environment without adherent conditions, are able to agglomerate into 3D spheroids to seek for support, forming embryoid bodies, which leads to spontaneous differentiation of undifferentiated cells into cells from one of the three-primary germ layers<sup>67</sup>. With the discovery of the ROCK inhibitor, it was a great step to explore the potential of these aggregates to maintain their pluripotency and proliferative capacity<sup>59</sup>, overcoming the problems imposed by physical supports like the microcarriers, since there is no requirement of attachment surfaces, adhesion molecules or hydrogels, because the cells simply attach to one another. This fact also allowed to solve problems of downstream processing of their production and cost reduction<sup>90</sup>.

However, even if the process of aggregation is not fully understood, the initial conditions and long-term maintenance of the desired quality of the aggregates in suspension is still an issue to be settled, since the slightest change might be responsible for a different phenotype in the end<sup>91</sup>. It was previously shown already that the use of controlled techniques such as forced agitation, micro-contact patterning and the used of bioreactors with continuous agitation is capable of influence the aggregates morphology and minimize heterogeneity<sup>92</sup>.

Another type of culture, the hanging drop method, which enables the formation of embryonic bodies in a droplet-like culture in which the aggregates are formed, is also an option to simulate a micro-environment in a 3D static culture. This technique cannot contribute for a scaling-up process, though it certainly helps contouring the issues of developing central necrosis of larger aggregates, typically formed in dynamic cultures, and can be used as *in vitro* assays for drug screening<sup>93</sup>.

In suspension, these cells rely on the interdependent way different molecules have to adhere to one another. These include cell adhesion molecules (CAMs), including connexins, multimeric transmembrane proteins from gap junctions, that participate in cell-cell communicating<sup>94,95</sup>, tight junctions, which prevent the leakage of components from the cells and from their metabolism, and E-cadherin, a characteristic cell cycle protein. As for the latter, this has shown to play an important role, not only on the cellular adhesion, but also in the overall biology of the cells by regulating their cellular homeostasis and also maintaining the self-renewal capacities of the cells, as well as their proliferation<sup>96</sup>, and on iPSCs reprogramming<sup>97</sup>.

Within the morphology of the aggregates, size is extremely relevant regarding the final product. It had been previously shown in the case of mouse embryonic bodies (mEBs) with size around 500  $\mu\text{m}$  are more prone to derivate into cells from the mesoderm and endoderm, while aggregates with a diameter around 110  $\mu\text{m}$  tend to originate cells of the ectoderm<sup>98</sup>. If the aggregates formed have a diameter of about 200  $\mu\text{m}$ , it would lead more easily into forming definite ectoderm, while large ones (around 1200  $\mu\text{m}$ ) would lead into forming mesoderm<sup>99</sup>.

The way these aggregates behave in a culture can be studied under different conditions, regarding the type of medium used, the culture time or under static and dynamic circumstances.

#### **1.3.4.3.1. Aggregate-based 3D Static Cultures**

In order to promote this spherical shape form characteristic of embryonic bodies *in vivo*, it was necessary to design new vessels that could meet these standards. In an attempt to avoid the shear stress typical from bioreactors, but maintaining the volumetric shape of the aggregates, dishes with wells small enough to hoard the cells and to enhance their development were created. These microwells have a magnitude of ten to hundreds of micrometres and are able to house a single 3D cellular aggregate promoting a defined size and uniform shape<sup>100</sup>. Each one of these wells works as a microenvironment that helps regulating the cellular growth and the development of a specific ECM architecture that 2D systems cannot, assuring their survival and proliferation<sup>101</sup>.

Three-dimensional static environment might be the right solution depending on the final objective. For example, it was shown how the signalling in the aggregates made from mouse embryonic stem cells (mESCs) in a 96-well plate allowed the obtention of satisfying optic-cup morphogenesis by gaining neural retinal tissue, as seen *in vivo*, with great reproducibility<sup>102</sup>. The aggregates self-organized intrinsically involving stepwise and domain-specific regulation of local epithelial properties. This environment also permitted the study of the aggregation of neural rosettes, which can be close to reality *in vivo* of the formation of the neural tube, and the abnormalities that appeared could be an indicator of neurotoxic effects during the embryonic development<sup>103</sup>.

Obviously, the type of vessel contributes largely to the morphology and development of the aggregates. Vessels designed with a specific lithography and non-adherent materials such as poly(dimethylsiloxane) (PDMS) or poly(ethylene glycol) (PEG) will promote the formation of the aggregates and influence how they will be developed. These vessels usually are composed of microwells that enable a high-throughput formation of PSCs aggregates from one single-cell<sup>104</sup>. It is expected that each well will hold one single aggregate to fully analyse their development. The three-dimensional geometry of the wells promotes the three-dimension aggregation of the cells.

These wells could also take various shape, either rectangular or cylindrical, though it had been previously developed a PDMS-based concave microwell dish which showed to promote more spherical and homogenous aggregates of ESCs, as well as the width of the well which was also a determinant factor for the differentiation of the cells, since the process is size-dependend<sup>105</sup>. Being size-dependend

implies that aggregates which are too small in diameter tend to compromise the cells survival due to the lack of support, though aggregates too large will restrict the access of the medium components to the inner cells of the aggregates, contributing for the heterogeneous development of the aggregate and leading to their death posteriorly, as previously tested in V-bottom wells<sup>106</sup>.

Nevertheless, limitations regarding these systems are still part of the global equation. Static environments cannot simulate *in vivo* conditions perfectly, such as the bloodstream, cellular oxygenation, and nutrition and waste removal occur by diffusion, hence the need for the pores to be millimetre-sized to create a microenvironment that can regulate better the cells' maintenance. Dynamic systems, however, can overcome this issue by facilitating the exchange of the previously mentioned topics<sup>101</sup>. Moreover, new, and more importantly, commercially available scaffolds for the growth of hPSCs are yet to be developed, regarding the improvement of characteristics such as stiffness, porosity, biocompatibility and responsiveness to enzymatic activity without compromising other parameters<sup>101</sup>.

#### **1.3.4.3.2. Aggregate-based 3D Dynamic Cultures**

Three-dimensional cultures permit to closer meet reality, and dynamic environments are the answer for the production of larger amounts of cells for future applications<sup>75,85</sup>.

In order to create the ideal environment for the large-scale production of these cells, several aspects should be taken into account. A fully operational and controlled system of the culture conditions and biochemical and biophysical parameters, with the optimal agitation speed to control the aggregates size, which permits the homogeneity of the suspension and enhances mass transfer, can be achieved using 3D dynamic cultures such as bioreactors<sup>91</sup> (Figure 8).

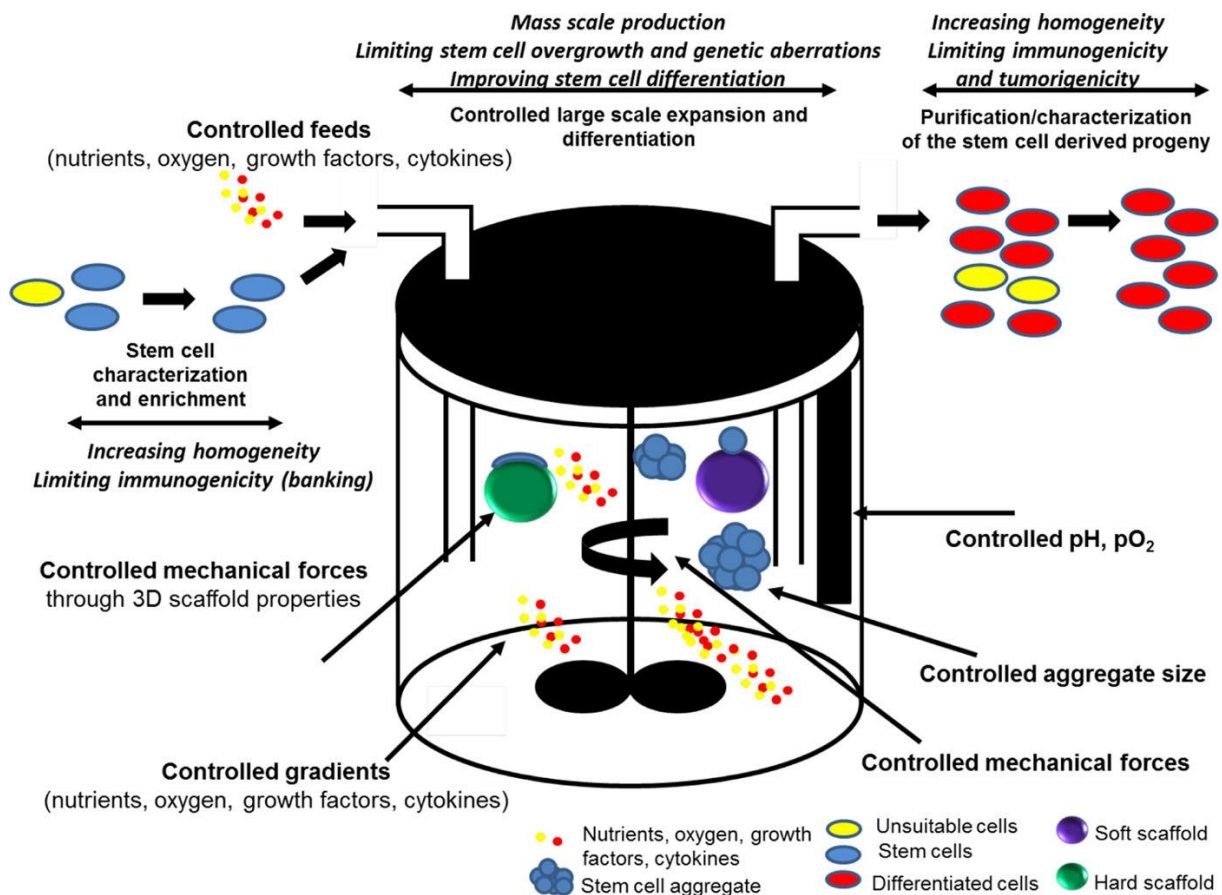


**Figure 8 - Illustration of a bioprocess engineering approach with bioreactors to alleviate current limitations in the use of stem cells for clinical application.** Bioreactors enable the large-scale stem cell expansion and differentiation in a controlled environment. They also allow to control the mechanical forces, feeds, and gradients of nutrients and growth factors, pH, oxygen, as well as the aggregate size. With the detailed characterizations of input cells and output cells, the homogeneity of the produced cell population will be increased. (Adapted from Sart *et al.*<sup>97</sup>).

As shown before, various types of bioreactors have been studied regarding their advantages and disadvantages and the final aim. Stirred-tanks bioreactors with continuous agitation are favourable to attenuate gradients of media components, and their impellers are also responsible for modelling the aggregates shape and size as cells collide into each other<sup>108</sup>.

Furthermore, it was shown before that mechanical forces applied to fibronectin or laminin to integrin receptors increased cell spreading and stiffness, but decreased their proliferation rate and their pluripotency, shown by the downregulation of the OCT3/4 marker. However, when applied to E-cadherin (Cdh1), no effects were shown on cell spreading, pluripotency and self-renewal of mouse ESCs, even if cell stiffening was increased<sup>109</sup>. E-cadherin and pluripotency of the cells can decrease with the inhibition of myosin IIA when prolonged hPSCs contraction happens. With that being said, mechanical stimulus by agitation can enhance cell contraction at the apical part of the cells, temporally activating myosin IIA and sustaining E-cadherin and the cells' self-renewal<sup>110</sup>.

Regarding differentiation, the process of expansion and maintenance of the cells, and differentiation itself are still two separated issues, therefore, moving towards a method that can accomplish both of them in 3D aggregates sequentially would be a milestone to be achieved<sup>91</sup>.

Contrarily to what happens in 3D static conditions, mechanical stress is present in dynamic bioreactors and it tends to increase with the scaling-up. Moreover, it limits the creation of a microenvironment that allows the high-throughput of the results, therefore the experiments are often performed and improved by trial and error, and the analysis of the state of the culture has to be done at a population level or by sampling, instead of single aggregates<sup>91</sup>.

In the future, it is expected that 4D methods will be implemented, which will allow real-time hPSC aggregates monitoring and the understanding of the effect of key metabolites in the culture to further promote support the robustness of the scaling-up process, which has yet to be developed, even at laboratory scale<sup>111</sup>.

## 2. AIM OF THE STUDIES

Human pluripotent stem cells have promising characteristics that have been motivating their exhaustive research. Obviously, not only it is of great interest to discover new ways to safely apply these cells in engineering, medicine and other related fields, but it is also a constant worry how to maintain and, most importantly, how to guarantee the precise quantity and quality of these cells, anytime and anywhere in the World. The step from the laboratory scale to the industrial one, to latter be used in clinical treatments, demands a perfectly robust and reproducible culture system, with xeno-free and chemically defined mediums, free from contaminants, while ensuring good manufacturing practises at all times. Therefore, the standardization of the current developed processes is a constant need in this field of technology.

The aim of this work is to study the divergence that occurred between two stocks of the same line of hiPSCs, 1383D2, that will affect future experiments. In order to do that, the effect of the exposure of these cells to the ROCK inhibitor was studied, while being cultured in 2D static conditions, with the ROCK inhibitor for 24 hours, and in 3D static and dynamic ones, with the ROCK inhibitor for 96 hours and 120 hours, using the xeno-free medium, StemFit®, in all cases. Culture parameters such as cell density, attachment efficiency, live cell ratio, specific growth rate, apparent specific growth rate and aggregates' diameter were collected to further take conclusions about the behaviour of these cells by comparing them to other stock of cells from the same line. Images were captured using phase contrast microscopy, bright field microscopy and confocal microscopy for the determination of these parameters and for studying the morphology of the cells from both cultures. An immunostaining technique was also applied to conclude about the robustness of these aggregates.

## **3. MATERIALS AND METHODS**

### **3.1. Cell Culture**

#### **3.1.1. Cell line**

The hiPSC line used, 1383D2, was kindly provided by CiRA (Center for iPS Cell Research and Application, Kyoto University), on behalf of this study. This line was maintained and kept stable using a shorter fragment of laminin-511, named laminin-511 E8 fragment (LN511E8), which, when recombinantly expressed, is isolated more easily and with a greater yield and purity than full-length laminin-511. When conjugated with a completely xeno-free medium such as StemFit<sup>®</sup>, hiPSCs can be easily stabilized and passaged by individualizing the cells for long periods, without karyotype abnormalities<sup>38</sup>.

#### **3.1.2. Culture media**

In the present work, it was used the StemFit<sup>®</sup> Basic02 medium (Ajinomoto, AK02N), a defined, xeno-free medium for the culturing of the hiPS cells. It is divided into three components named “Liquid A”, “Liquid B” and “Liquid C”. The first one is stored at 4°C, while the other two are stored at -20°C. Both should be thawed before being used at room temperature and by adding 50 mL of “Liquid B” and 2 mL of “Liquid C”, to 450 mL of “Liquid A”, under aseptic conditions, to complete the medium preparation.

## **3.2. Culture Preparation**

#### **3.2.1. Cells' Maintenance**

In a 100-mm dish, 5 mL of DPBS (Dulbecco's phosphate-buffered saline) was added before adding 27.5  $\mu$ L of the coating solution, containing 175  $\mu$ g of iMatrix-511 (nippi Atrixome), previously dissolved with 350  $\mu$ L of distilled water. After the addition, the vessel was shaken carefully in order to spread the solution evenly on the surface. The dish was then incubated at 37°C and with 5% of CO<sub>2</sub> for one hour. Afterwards, the solution was discarded and 5 mL of StemFit<sup>®</sup> AK02N with 10  $\mu$ M ROCK inhibitor (Y-27632) was added before returning to the incubator. Precultured cells were then seeded into this plate, as described in 3.2.2. Cell Harvesting and Passaging.



### 3.2.2. Cells' Harvesting and Passaging

As referred before, these cells need to attach to both a surface and to each other for support and proliferation. When harvesting these cells, it is common to use enzymatic methods to promote the cell-substrate and cell-to-cell dissociation.

The obtention of cells for culturing was proceeded by first discarding the medium from the hiPSC culture growing in a 100 mm tissue culture-treated culture dish (Corning Inc.). In 2D culture, cells were passaged when the initial seeding density was  $2.50 \times 10^3$  cells/cm<sup>2</sup>. The plate was washed with 5 mL of DPBS (Sigma-Aldrich®) and then discarded again to guarantee the full removal of the wasted medium. Afterwards, 3 mL of 5mM EDTA (Dojindo Molecular Technologies, Inc.) mixed with 3  $\mu$ L of 10  $\mu$ M ROCK inhibitor (Y-27632, FUJIFILM Wako Pure Chemical Corporation, 251-00514) was added into the plate for 10 minutes. After this time, 3 mL of TrypLE™ 1X (Gibco®, ThermoFisher Scientific), that uses EDTA as chelator and has no addition of phenol red, mixed with 3  $\mu$ L of ROCK inhibitor, was added to the plate. After 7 minutes, the detachment of the cells was observable under the phase contrast microscope CKX53 (OLYMPUS®), and they were gently detached by pipetting. From a previously prepared 10 mL of fresh StemFit® mixed with 10  $\mu$ L ROCK inhibitor, it was drawn 3 mL of the mixture and added to the plate, after complete detachment of the total amount of cells. Then, the total volume of the dish was transferred into a 15 mL Falcon tube (ThermoFisher Scientific™), before another 3 mL of the medium with ROCK inhibitor was added to collect the remains of the cell suspension still in the dish. The tube was centrifuged for 3 minutes at a speed of 170 x g. The supernatant was discarded and 1 mL of StemFit® with ROCK inhibitor was added once again, cells were rinsed by pipetting before another 2 mL were added. Aliquots of 50  $\mu$ L were collected into Eppendorf tubes and diluted with 50  $\mu$ L of DPBS before being counted using the Trypan Blue Exclusion method and the Automated Cell Counter.

### 3.2.3. Cells' Counting

In 3D culture, at  $t = 24$  h and  $t = 96$  h, aliquots of 500  $\mu$ L were collected into Eppendorf tubes from both the bioreactor and the wells of the dimple plates, after rinsing and collecting the aggregates into 15 mL tubes, in the case of the dimple plates. Each Eppendorf was centrifuged for 1 minute, the supernatant was discarded and 500  $\mu$ L of Accumax™ (Innovative Cell Technologies, Inc.) was added to break the aggregates into single cells, before being incubated for 10 minutes. After this time, cells were pipetting to further promote the breakage of the aggregates into individual cells, before being centrifuged once again for 1 minute. The Accumax™ compound was then discarded and PBS (phosphate-buffered saline) was added before counting as followed: 50  $\mu$ L, at both initial seeding time ( $t = 0$ ) and at  $t = 24$  h, or 100  $\mu$ L, at  $t = 96$  h. Single cells were counted using the Trypan Blue Exclusion method and using an TC20™ Automated Cell Counter (Bio-Rad). The automated cell counter was set in to detect cells with a diameter within 8 to 30  $\mu$ m, and it works with a cell density range from  $1.00 \times 10^5$  to  $5.00 \times 10^6$  cells/mL. Knowing the working volume of the vessel, in mL, in which the cells would be then seeded, the initial cell density, in cells/mL, the dilution factor, due to the addition of PBS, and

the average of cell counting, in cells/mL, using every sample, it was possible to calculate the seeding volume, in mL, which can be represented by equation (1).

$$\text{Seeding Volume (mL)} = \frac{\text{Working Volume (mL)} \times \text{Initial Seeding Density (cells/mL)}}{\text{Dilution Factor} \times \text{Average Cell Counting (cells/mL)}} \quad (1)$$

### 3.2.4. Culture Inoculation

In the scope of the present work, it was relevant to understand the cells' behaviour in at least three different environments, in order to understand what would be the best conduct to adopt in the future.

#### 3.2.4.1. 2D Static Conditions

To study the cells under 2D static conditions, two 8-well culture plate (Thermo Scientific™ Nunc™ Cell-Culture Treated Multidishes) were used, in which only four wells from each plate were used, each well with a total working volume of 3 mL. For the eight wells, it was prepared the coating solution, containing 42  $\mu\text{L}$  of iMatrix and 12 mL of PBS, from which 1.5 mL were added to each well. The vessels were then shaken to homogeneously spread the coating solution, before incubating the plates at 37°C and 5%  $\text{CO}_2$  concentration for an hour. At  $t = 0$ , the procedure for harvesting the precultured cells at an initial seeding density of  $2.50 \times 10^3$  cells/cm<sup>2</sup> and seeding them into the designated wells was as described in 3.2.2. Cells' Harvesting and Passaging. To harvest the cells from these wells for counting, the technique used was the same as it was described, although the quantities of the reagents had a slight change: instead of 3 mL from each reagent, it was used 1 mL per well. The culture was maintained for a total of 120 hours, and the medium was changed every 24 hours, adding 2.1 mL per well. The ROCK inhibitor was added at  $t = 0$ , and not added anymore after the first medium change, at  $t = 24$  h. To count the cells and estimate the cell density, the culture from one of the plates was used at  $t = 72$  h, while the second one was used at the end of the culture time, at  $t = 120$  h.

#### 3.2.4.2. 3D Static Conditions

To study the formation of aggregates in a three-dimensional setting without agitation, 6-well dimple plates (Elplasia™, Kuraray Co., Ltd.) were used. Two different dimple plates in which the first plate, used at  $t = 24$  h for counting and discarded afterwards, contained two wells for culturing the cells at initial density of  $1.00 \times 10^5$  cells/mL, one with ROCK inhibitor (10  $\mu\text{M}$ ) for 48 hours, until when it was performed the first medium change, and the other one with it for 96 hours. As for the second plate, whose wells underwent the same ROCK inhibitor treatment and left untouched, apart from when mthe

edium was changed, from  $t = 0$  until  $t = 96$  h, was used for counting at the latter referred time. Each well had a working volume of 6 mL of medium and the calculated volume of cells were seeded into it before being incubated at 37°C and 5% of CO<sub>2</sub>. The medium change was performed at  $t = 48$  h and at  $t = 72$  h.

When counting the cells, 3 mL from each well were first carefully discarded. From the remaining 3 mL, around 800 µL were used to rinse and then collect the aggregates that were formed inside the dimples. The progression of the aggregate collection was followed under the microscope, adding PBS until all of the aggregates were collected into a 15 mL Falcon tube. The total volume collected from each well should not have exceeded the initial working volume of 6 mL per well. Counting was performed as previously described in 3.2.3. Cells' Counting.

### **3.2.4.3. 3D Dynamic Conditions**

As to study the formation of aggregates in a three-dimensional environment with continuous agitation, cells at the initial density of  $1.00 \times 10^5$  cells/mL were seeded and then maintained in culture for 96 hours in a 30 mL disposable bioreactor (ABLE Corporation & Biott Co., Ltd). Two of these bioreactors were used, one in which ROCK inhibitor (10 µM) was present in the culture for 48 hours, before changing the medium for the first time, while in the other one it was maintained for the entire culture time. After seeding, the bioreactors were incubated at 37°C and 5% of CO<sub>2</sub>, with a continuous agitation of 55 rpm. The medium change was performed at  $t = 48$  h and at  $t = 72$  h. Counting was performed as previously described in 3.2.3. Cells' Counting.

## **3.3. Cryopreservation**

The preservation of the aggregates of cells was done at the end of the culture time of 96 hours, for both the dimple plate and the bioreactor.

Three samples of 500 µL were taken from each vessel into Eppendorf tubes, which were after vortexed for about 10 seconds and the supernatant discarded afterwards. Cells were carefully placed in between two layers of Tissue-Tek™ O.C.T. (Optimum Cutting Temperature) Compound (Sakura®), removing the excess of medium, and spreading the cells evenly. Cells were cryopreserved using liquid nitrogen (-196°C) and frozen at -80°C before sectioning.

## 3.4. Aggregates' Sectioning

The frozen aggregates were cut using the cryostat Leica Biosystems CM1850 in order to proceed with immunostaining later. The aggregates were first left for an hour at the temperature of -18°C to facilitate their sectioning. The aggregates were sectioned with a thickness of 10 µm and placed in a glass slide for the immunostaining.

## 3.5. Characterization of hiPSCs

In order to understand the differences encountered in both vessels and in all conditions, a set of parameters and characteristics were quantified and analysed.

### 3.5.1. Attachment Efficiency and Live Cell Ratio

Cell density at a certain time ( $X_t$ ) could be calculated using the data obtained from the automated cell counter.

As for rating the viability of the cells, it was possible to calculate the attachment efficiency, in 2D culture systems, ( $\alpha (-)$ ), or the live cell ratio, in 3D culture systems, ( $\alpha^* (-)$ ), using the same expression, as shown in equation (2).

$$\alpha (-) = \alpha^* (-) = \frac{X_{24}}{X_0} \quad (2)$$

In which  $X_{24}$  and  $X_0$  represent the cell density, in cells/mL, at  $t = 24$  h and  $t = 0$ , respectively.

In 2D culture, the cell density was determined at  $t = 24$  h by taking images and counting the cells using ImageJ from *Fiji* software, and calculating it by using equations (3) and (4).

$$X_t = \frac{N_{\text{live cells}}}{A_{\text{image}}} \quad (3)$$

$$X_t = \frac{[\text{Cells}] \times V_{\text{suspension}}}{A_{\text{well}}} \quad (4)$$

### 3.5.2. Specific Growth Rate and Apparent Specific Growth Rate

Furthermore, it was also possible to determine the growth and proliferation rate of the cells until they reached an exponential growth rate. The increase in cell population during this stage could be defined by equation (5).

$$\frac{dX}{dt} = \mu \cdot X \quad (5)$$

In which,  $X$  represents, once again, the cell density, in cells/mL;  $t$  represents the time, in h, and  $\mu$  represents the specific growth rate, in  $\text{h}^{-1}$ .

Thus, from equation (5) it is possible to obtain the expression that permits calculating the specific growth rate, which is given by equation (6).

$$\frac{dX}{dt} = \mu \cdot X \Leftrightarrow \frac{1}{X} \cdot dX = \mu \cdot dt \quad (6)$$

When the data is collected twice during the culture time, as for the case of 3D culture conditions, then, from equation (6), it is possible to obtain the apparent specific growth rate ( $\mu^{\text{app}}$ ), in  $\text{h}^{-1}$ , which was given by equation (7).

$$\mu^{\text{app}} = \frac{\ln\left(\frac{X_{96}}{X_{24}}\right)}{t_{96} - t_{24}} \quad (7)$$

In which again  $X_{24}$  and  $X_{96}$  represent the cell density, in cells/mL, at 24 hours and 96 hours, respectively, and  $t_{96}$  and  $t_{24}$  the time at  $t = 96$  h and  $t = 24$  h, respectively.

### 3.5.3. Aggregates' Diameter

At both  $t = 24$  h and  $t = 96$  h, 500  $\mu\text{L}$  samples were collected from both vessels and placed into a 6-well plate, together with 2 mL of PBS in order to capture images of the cells. The aggregates' diameter was measured using a bright field system, IN Cell Analyzer 2000 (GE Healthcare Life Sciences). The images were then analysed using the ImageJ software from *Fiji* image process package to determine the area of each aggregate. Knowing the area, the aggregate diameter could be measured according to equation (8).

$$d = 2 \times \sqrt{\frac{A}{\pi}} \quad (8)$$

In which  $d$  represents the aggregate's diameter, in  $\mu\text{m}$ , and  $A$  represents its area, in  $\mu\text{m}^2$ .

### 3.5.4. Aggregates' Morphology

As commented before, the ROCK inhibitor plays an important role in the survival of hiPSCs in culture, and also in the structure of their cytoskeleton. Therefore, it was also taken samples of 500  $\mu\text{L}$  from both vessels and placed into a 6-well plate, together with 2 mL of PBS to take images using phase contrast microscopy and to conclude about the shape, size and other visible characteristics that could lead to assumptions about which was the most efficient technique to be adapted regarding these cells.

### 3.5.5 Immunostaining

To all the previously sectioned aggregates placed in glass slides, it was added the volume that would completely cover the sectioned aggregates, usually quantities of about 200  $\mu\text{L}$ . It started by removing the Tissue-Tek™ O.C.T. compound by washing the samples three times with PBS, followed by one washing with 4% paraformaldehyde (FUJIFILM Wako Pure Chemical Corporation) for the fixation of the cells in a period of 10 minutes. After this time, it was discarded, washed twice with PBS and added the solution composed of 50  $\mu\text{L}$  Triton X-100 (Sigma-Aldrich®), 0.5% dilution, and 10 mL Mili-Q® (Mecrk Millipore). After 5 minutes, this solution was discarded, and the samples were washed using the dilution buffer which was composed of 40 mL from a previously prepared solution, named antibody dilution, containing 2.5 mL of Block Ace (DS Pharma Biomedical Co., Ltd.) and 47.5 mL of Mili-Q®, and 40  $\mu\text{L}$  of Tween® 20 (Sigma-Aldrich®). After discarding, the dilution buffer was added once again for 15 minutes, before it was discarded once again, and the Block Ace added for 90 minutes. During this time, the primary antibody solution could be prepared, containing the working volume of 200  $\mu\text{L}$  of the antibody dilution, 1  $\mu\text{L}$  of E-cadherin and 4  $\mu\text{L}$  of Ki-67, as seen in Table 2. After said time, the Block Ace was discarded, the samples were washed once with TBS (tris-buffered saline) and the solution of the primary antibodies was added. The samples were left overnight, ideally for 16 hours, in the fridge at 4°C.

In the following day, what was left was discarded and then washed once with the dilution buffer, before adding it again for 15 minutes. After this time, it was discarded, and TBS was added, also for 15 minutes. During this period, and in the darkness, the secondary antibody solution was prepared containing 200  $\mu\text{L}$  of the antibody dilution, 1  $\mu\text{L}$  of Alexa Flour® 594 anti-rabbit and 1  $\mu\text{L}$  of Alexa Flour® 488 anti-mouse, as checked in Table 3. This solution was then added for 1 hour after discarding the TBS. After this time, it was discarded, TBS was added again for 20 minutes, discarded, added for 10 minutes, discarded and finally added once again for another 10 minutes. During this sequential process,

the DAPI (4',6-diamidino-2-phenylindole) solution was prepared by mixing 200  $\mu$ L of PBS with 0.6  $\mu$ L of DAPI (initially with a dilution rate of 1:50, and then diluted again 3  $\mu$ L/mL). This solution was then added for 20 minutes after discarding the previous one. When done with this time, the DAPI solution was discarded and PBS was added and discarded according to the following sequence: washed twice, added for 10 minutes, discarded and then, right after adding for another 10 minutes, washed and finally discarded.

Two or three drops of *SlowFade* (ThermoFisher Scientific), an antifade reagent which extends the primary antibody action, were added before analyzing the results using a confocal laser scanning microscope, the FluoView FV1000 (OLYMPUS®).

**Table 2 - Primary antibodies' information regarding the type of host, clonality, reactivity, catalogue identity and supplier and working dilution.**

Primary Antibody	Host	Clonality	Reactivity	Catalogue Identity, Supplier	Working Dilution
<b>E-cadherin</b>	Mouse	Monoclonal (Clone 67A4)	Human, Rat	sc-21791, SCB	1:200
<b>Ki-67</b>	Rabbit	Monoclonal (Clone SP6)	Mouse, Rat, Human, Common Marmoset	ab16667, abcam	1:50

**Table 3 – Targeted primary antibodies' information regarding the type of host, clonality, reactivity, catalogue identity and supplier and working dilution.**

Targeted Primary Antibody	Host	Clonality	Reactivity	Conjugate	Catalogue Identity, Supplier	Working Dilution
<b>E-cadherin</b>	Goat	Polyclonal	Mouse	Alexa Flour® 488	A11001, ThermoFisher	1:200
<b>Ki-67</b>	Goat	Polyclonal	Mouse, Rat, Human, Common Marmoset	Alexa Flour® 594	A11012, ThermoFisher	1:200

# 4. RESULTS AND DISCUSSION

## 4.1. hiPSCs' Divergence

As previously explained in topic 1.3.2. Process Standardization, one of the top priorities in stem cells engineering is to fully understand the behaviour and characteristics of the cell line under study. This certainly includes the final establishment of protocols that would allow to obtain of cells with determined parameters of quantity and quality whenever and wherever it would be necessary.

Initially, it was studied what would be the optimal initial seeding density to culture the cells in a 30 mL bioreactor in order to establish a range of values that could be beneficial for future experiments. However, from the parameters collected only after 24 hours of culture, it was possible to undoubtedly conclude that cells from a specific stock have undergone a transformation process when comparing to the laboratory's data of the same line of cells from other stock.

Therefore, in the scope of this work, it was necessary to understand the behaviour of two different stocks of the same line of hiPSC, the 1383D2 line. It was of interest to understand and speculate how and why did this culture suffered changes comparing to another from the same hiPSCs line. By studying the behaviour of the cells in 2D (Figure 9) and 3D culture, under static and dynamic conditions (Figure 10), and understanding how the permanence of the ROCK inhibitor influenced the culture, it was possible to take conclusions about the best course of action to culture these cells in the future.

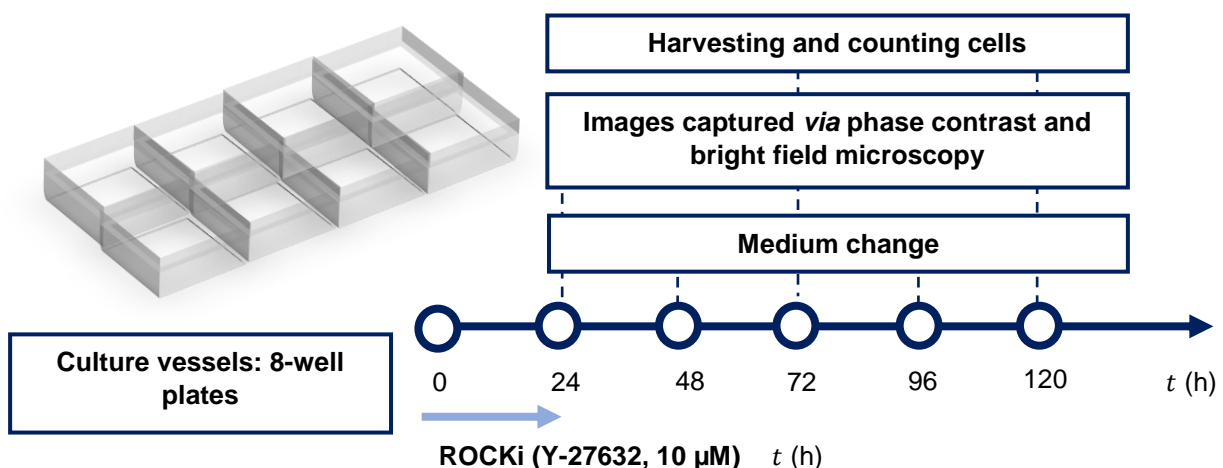


**Figure 9 - Overall design of the experiment.** hiPSCs were cultured in 2D static environment, using 8-well plates, with a culture time of 120 hours and ROCK inhibitor in the culture for 24 hours.



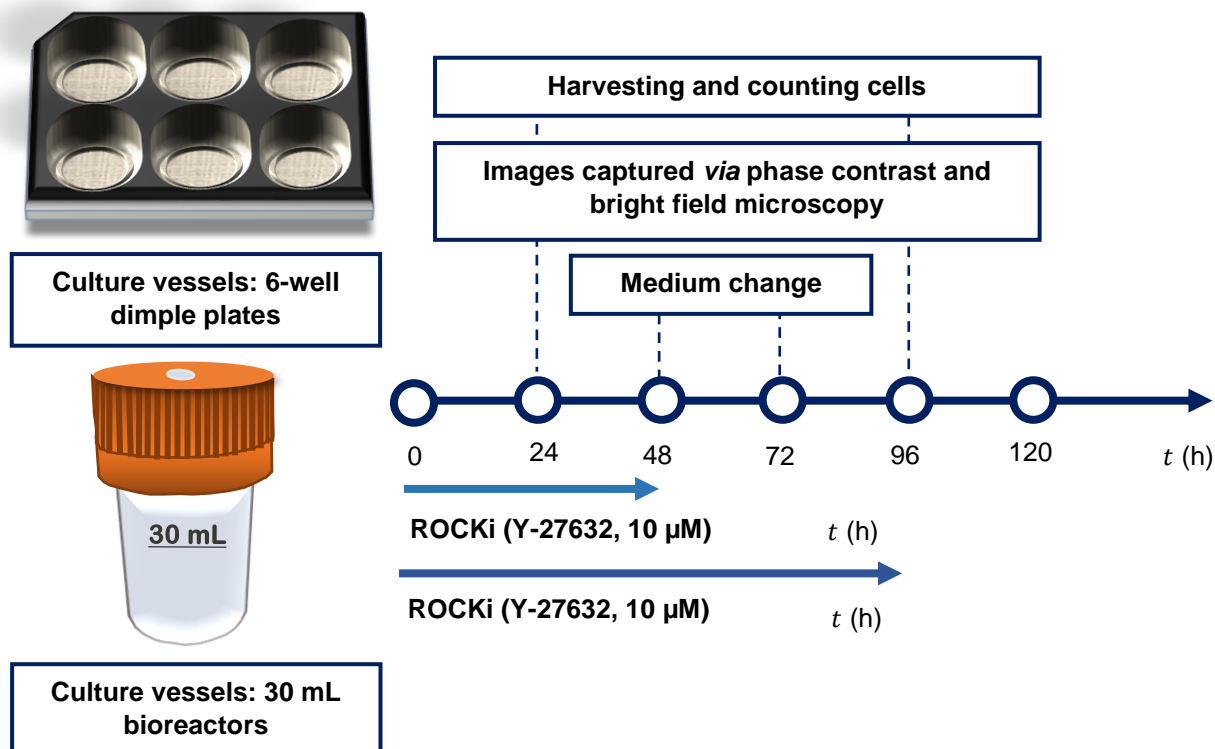


**Figure 10 – Overall design of the experiment.** hiPSCs were cultured in 3D static and dynamic environment, using 6-well dimple plates and 30 mL bioreactors, respectively, for a culture time of 96 hours and ROCK inhibitor in the culture for 48 and 96 hours.

Thus, and to better distinguish the type of cells throughout the present work, to the stock with no issues or modifications of any kind, it was given the name “Type A”, while the cells which were suspected to have undergone changes, were named “Type B”. In order to understand their behaviour, different variables were studied, and images were collected to better assess what would be the best strategy to adopt when working with these cells, while maintaining their undifferentiated state. It was also necessary to understand the differences that were possible to observe depending on the type of culture system they were inserted into. Data from two-dimensional and three-dimensional cultures were collected regarding the cells attachment efficiency, in 2D, or live cell ratio, in 3D, specific growth rate, apparent specific growth rate, aggregates’ diameter and morphology to further take conclusions about Type B cells’ state.

## 4.2. Culturing in 2D Environment

Cells were cultured for 120 hours in 8-well plates, using the StemFit® medium with the ROCK inhibitor present in the first 24 hours of the culture. At seeding time, Type A cells could be described as having a spherical, until they attach to the surface, becoming mainly bilaterally branched, as seen in Figure 11A, after 24 hours. When forming colonies, the cells have a spherical shape in the centre of the colonies and they are branched in the periphery of it. The colonies were usually large and their shape

irregular at the end of the culture time (Figures 11B and 11C). Similar phenotypical characteristics were observable in Type B cells, as seen in Annex I.

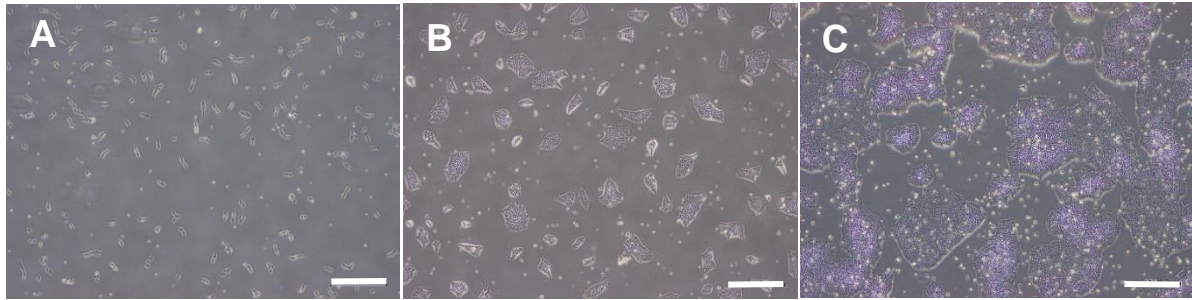


**Figure 11 - Images captured using phase contrast microscope of hiPSC for Type A cells.** Images were taken at **(A)**  $t = 24$  h, **(B)**  $t = 72$  h and **(C)**  $t = 120$  h. Dead cells correspond to the yellow floating spheres ( $n = 1$ ). (Scale bars =  $500 \mu\text{m}$ ).

The specific growth rate ( $\mu$ ) could be calculated using equations (6) and (9). Since data was collected at  $t = 24$  h,  $t = 72$  h and  $t = 120$  h, it was possible to draw the graph as it is represented in Figure 12, from which it is possible to determine the value for  $\mu$ .

$$\text{Cell Density, } X \text{ (cells/cm}^2\text{)} = b \times e^{\mu \text{ (h}^{-1}\text{)} \times t \text{ (h)}} \quad (9)$$

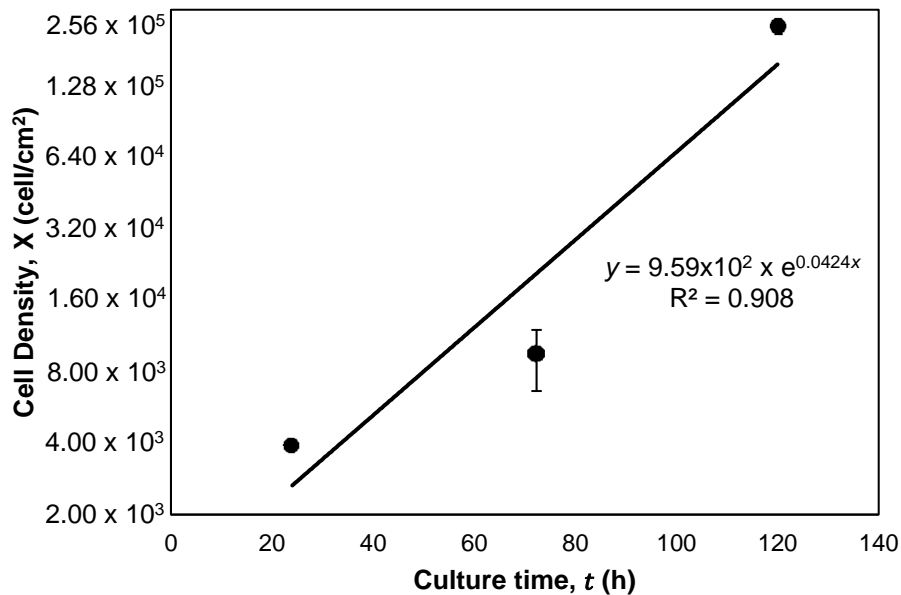


**Figure 12 - Growth curve for the Type A culture in 2D static conditions.** The graphic was plotted using a semi-logarithmic scale on the y-axis, at  $t = 24$  h,  $t = 72$  h and  $t = 120$  h. The error bars represent the standard deviation ( $n = 3$ ).

Cells cultured under the same conditions, for 120 hours and with the ROCK inhibitor for 24 hours, for both cells from Type A and Type B, presented the results for the attachment efficiency and the specific growth rate as calculated from equation (2) and equation (8), respectively. These parameters are shown in Table 4, for both types of cells.

**Table 4 – Growth kinetics parameters, the attachment efficiency ( $\alpha$ ) and the specific growth rate ( $\mu$ ), for Type A and Type B cells, in 2D static culture.** The values represented are the average at  $t = 24$  h and  $t = 120$  h, respectively, for the condition of study of the effect of the ROCK inhibitor in the culture for 24 hours, followed by the standard deviation ( $\pm$ ). Type B cells' unpublished results were kindly provided by laboratory members ( $n = 1$ ).

	24 h ROCK Inhibitor			
	$\alpha$ (-)		$\mu$ ( $10^{-2} \text{ h}^{-1}$ )	
	Type A Cells	Type B Cells	Type A Cells	Type B Cells
2D Static Culture	$1.54 \pm 0.00$	$1.38 \pm 0.09$	$4.24 \pm 0.35$	$5.00 \pm 0.00$

Interestingly, from the results in Table 4, it was demonstrated that both the  $\alpha$  and the  $\mu$  from the Type B cells were not drastically different when comparing to Type A cells.

From these results, it was possible to observe that the  $\alpha$  values from Type B, of  $1.38 \pm 0.09$ , is slightly lower than Type A cells', of  $1.54 \pm 0.00$ , even though it is still within a range of 10% discrepancy. As for the  $\mu$  value, the discrepancy is a bit higher, but not enough to be alarming and compromise the culture in any way. Actually, the variation might be due to technique differences of the operator, since in Annex II, the data provided by the laboratory members, it is possible to observe that, for the same cells, namely Type A cells, the specific growth rate value was  $(4.91 \pm 0.00) \times 10^{-2} \text{ h}^{-1}$ , which is similar to Type B cells'.

This might show that the physical stress and aggregate formation are both factors that might have a strong influence in the proliferation of these Type B cells compared to the Type A cells. In the conventional 2D system culture, and as in this case, cells are grown in dishes coated with ECM components, which will aid to their attachment since the moment they are seeded into the vessel. This 2D culture brings a stable environment for the proliferation of cells from Type B, although, and as referenced before, it is widely known that 2D culturing limits greatly the scalability of some processes.<sup>69</sup>

## **4.3. Effect of the Exposure to ROCK Inhibitor in 3D Culture**

As commented before, it was aimed to understand how the ROCK inhibitor would contribute to the survival, maintenance and proliferation of Type B cells. Therefore, it was tested if the time of exposure of the ROCK inhibitor would or not be beneficial to these cells, as well as to understand how it could contribute for their sustainability when forming aggregates, in both 3D static and dynamic culture and finally how the morphology of the aggregates varied regarding the time exposure to the ROCK inhibitor and the type of vessel used.

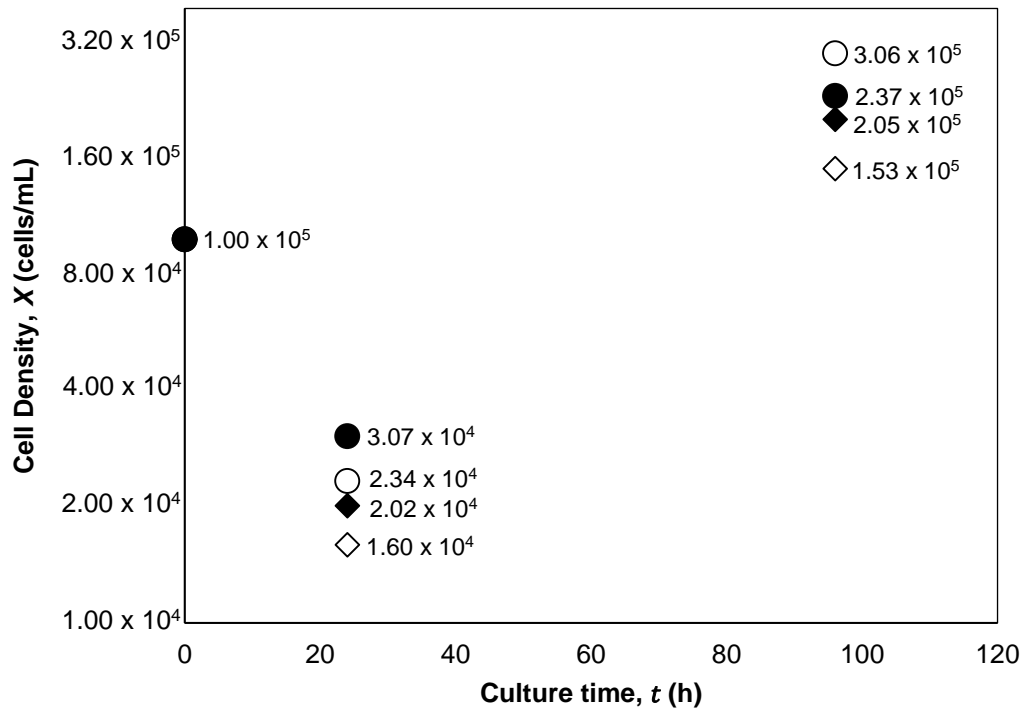
### **4.3.1. Influence of Exposure Time to ROCK Inhibitor**

As a first approach, it was thought that the time of cell exposure to the ROCK inhibitor in the culture would contribute largely to the survival and proliferation of these cells in a 3D culture environment.

Cell growth was maintained for a total of 96 hours, in 6-well dimple plates, that simulate static conditions, and in 30 mL bioreactors, with continuous agitation of 55 rpm. Despite the number of wells, two dimple plates were used in order to minimize the risk of contamination and to avoid non-homogenous aggregate formation inside the dimples from moving the plate more times than it was necessary.

In both culture systems, it was studied the exposure of the ROCK inhibitor in the culture for 24 hours and 96 hours (the total culture time).

The variation of cell density measured using the automated cell counter at  $t = 24$  h and  $t = 96$  h, for both the dimple plates and the bioreactors, under the effect of the ROCK inhibitor for the time length of 48 hours and 96 hours, is represented Figure 13.



**Legend:**

- 48 h ROCKi in 3D Static Culture
- 96 h ROCKi in 3D Static Culture
- ◆ 48 h ROCKi in 3D Dynamic Culture
- ◇ 96 h ROCKi in 3D Dynamic Culture

**Figure 13 - Variation of Type B cells' density in both 3D static and dynamic cultures with different exposure times to the ROCK inhibitor.** Graphic plotted in a semi-logarithmic scale on the y-axis at seeding time ( $t = 0$ ),  $t = 24$  h and  $t = 96$  h, for the condition of study of the effect of ROCK inhibitor in the culture for 48 hours and 96 hours ( $n = 1$ ).

In Figure 13 it is possible to observe an overall drop in the values of cell density, a clear indication of the adversities that Type B cells have to go through to adapt to the new domain, regardless of the type of vessel used. Despite of the culture system used, at  $t = 24$  h, the exposure time of the cells to the ROCK inhibitor was exactly the same, so the cell density value between the static cultures and the one between the dynamic cultures should be exactly the same. The discrepancy of results, however, might be due to the handling technique and the time gap between the detachment of the cells and the seeding into the designated culture vessels to be then incubated.

Even so, it was possible to observe the cell density practically doubled when comparing the static culture to the dynamic one with the ROCK inhibitor for 96 hours, which is a good representation of the adaptation turnover of the cells after passaging and seeding into the new vessels and incubated for more than 24 hours.

Moreover, even though the size of the aggregates is a morphological characteristic, it was also an aspect that was thought to be related to the duration of exposure of the cells to the ROCK inhibitor. Therefore, samples from each culture vessel were collected and images were captured using bright field microscopy. By using the ImageJ software, it was possible to calculate the area of the aggregates and, therefore, their diameter, by using equation (8). The vertical scatter plots of the results obtained are represented by Figures 14 and 15.

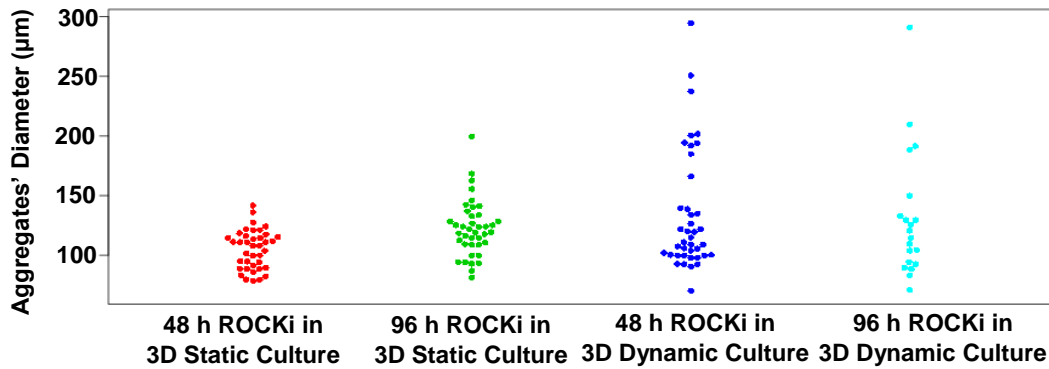


**Figure 14 - Variation of the aggregates' diameter.** Data collected at  $t = 24$  h, in both 3D static and dynamic culture, for the conditions of study of the effect of ROCK inhibitor in the culture for 48 hours and 96 hours ( $n = 1$ ).

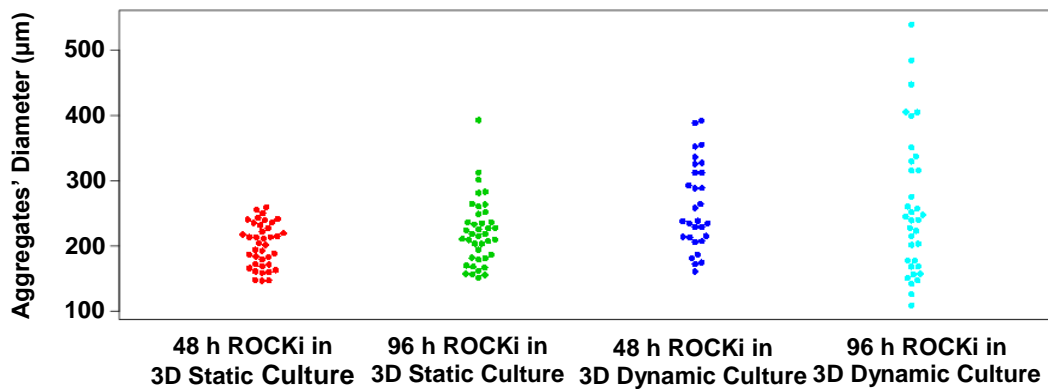


**Figure 15 - Variation of the aggregates' diameter.** Data collected using at  $t = 96$  h, in both 3D static and dynamic culture, for the conditions of study of the effect of ROCK inhibitor in the culture for 48 hours and 96 hours ( $n = 1$ ).

From the results, the first conclusion that could be observable even to the naked eye was that Type B cells can form lasting aggregates, whose the diameter increased as the culture times proceeded from the 24 hours analysis to the 96 hours analysis. After one day, the dynamic culture presented, not only a bigger dispersion of diameter results, but also higher values, when comparing to the static culture.

However, the higher density of the results revealed to be between 75 and 150  $\mu\text{m}$  in all cases (Figure 14).

After 96 hours, it was possible to conclude two different aspects, regarding the dimension of the aggregates and the time dependency.

Firstly, and once again, the dynamic culture overcame the static culture in terms of aggregate size (Figure 15). Even if in 3D static conditions shows to have extensive agglomeration, it is still lesser than the dynamic one, as expected<sup>57</sup>. This is a valuable aspect to be taken into consideration for future applications, since large numbers of cells are usually required for most of the regenerative medicine or tissue engineering applications<sup>34</sup>. The formation of larger aggregates in 3D dynamic culture could mainly have been due to the agitation of the bioreactors which promote the collision of the cells more efficiently and, thus their attachment to each other too. Also, surely that the continuous agitation promotes the collision among the cells, but also among the aggregates, as the culture time proceeds. This dynamics between the collapse and coalescence of the aggregates will influence the cells' proliferation rate as the culture develops and the fate of their deviation. This merging of the aggregates also explains the smaller number of aggregates in the samples used to get the images, analyse and later draw the vertical plots represented in Figures 14 and 15.

Secondly, it is possible to observe the size discrepancy, regarding day 1 and day 4 analysis, and also the different type of culture systems. After the first 24 hours the aggregates' size was not larger than 300  $\mu\text{m}$ , contrarily to after 96 hours of culture. It is curious to notice that the presence of the ROCK inhibitor for 48 hours or for the entire culture time barely brought any effect to the aggregate size in the case of the static culture, since the higher density of samples is confined between sizes 150 and 300  $\mu\text{m}$ . However, the same was not entirely true in the dynamic culture, since the extended permanence of the ROCK inhibitor showed to lead to a wider range of values and also to a beneficial increment of the diameter of the aggregates, an aspect to consider in future research. This could reinforce the hypothesis that altered cells like the ones from Type B have trouble adapting and adjusting to the dynamic culture and that the ROCK inhibitor might bring an advantage to their culturing.

### 4.3.2. Static and Dynamic Conditions

In order to further understand the variances in the different cultures, it was calculated two growth kinetics parameters, namely the live cell ratio ( $\alpha^*$ ) and the apparent specific growth rate ( $\mu^{\text{app}}$ ), for static and dynamic conditions, with the ROCK inhibitor in the culture for 48 hours and 96 hours, for both cell types (Table 5). The unpublished results regarding Type A cells for comparison to Type B cells were kindly provided by members of the laboratory for the purpose of the present work.

**Table 5 - Growth kinetics parameters, the live cell ratio ( $\alpha^*$ ) and the apparent specific growth rate ( $\mu^{app}$ ), for Type A and Type B cells, in 3D static and dynamic culture.** The values represented were collected at  $t = 24$  h and  $t = 96$  h, for the condition of study of the effect of ROCK inhibitor in the culture for 48 hours and 96 hours. Type A cell's results for 3D dynamic culture with the ROCK inhibitor for 48 hours are followed by the standard deviation ( $\pm$ ). Type A cells' unpublished results were kindly provided by the laboratory members ( $n = 1$ ).

		$\alpha^*$ (-)		$\mu^{app}$ ( $10^{-2} \text{ h}^{-1}$ )	
		Type A Cells	Type B Cells	Type A Cells	Type B Cells
48 h ROCKi	3D Static Culture	0.55	0.61	3.00*	2.84
	3D Dynamic Culture	$0.67 \pm 0.04$	0.20	$2.30 \pm 0.06$	3.22
96 h ROCKi	3D Static Culture	-	0.47	-	3.57
	3D Dynamic Culture	-	0.16	-	3.14

\*Calculated value from 24 – 120 h

These parameters permit to evaluate the culture as it develops, providing an understanding of the quality of the cells right after the first 24 hours.

The live cell ratio was determined after 24 hours in all cases, and so was the time exposure of the cells to the ROCK inhibitor in the cultures. Again, and as previously exposed by Figure 13, the values between the dynamic cultures and the static cultures should be exactly the same in theory, but experimental errors and timing might have contributed for the small variation in the values.

Nevertheless, regarding the results for the live cell ratio, if the value varied between 0 and 1, it was possible to observe that, the Type B cells' survival was largely compromised in the dynamic culture, since the success rate was only 20% and 16%, when comparing to the static culture, which was 61% and 47%. When comparing the value to Type A cells, it was possible to conclude once again that there were no drastic changes in the  $\alpha^*$  value in the case of the dimple plates, since the value increases from 0.55 to 0.61, but cell apoptosis seemed to have been aggravated in the case of dynamic culture, where Type B cells had a survival ratio of 20%, comparing to Type A, which was 67%. In Annex III, even if with different conditions, such as culture time of 120 hours and ROCK inhibitor exposure of 24 hours and 120 hours, it is possible to observe that the live cell ratio is above 60% for Type A cells grown in 3D dynamic culture. In Annex IV, even if the culture time was of 120 hours and the exposure time to the ROCK inhibitor of 24 hours, it is possible to observe that the live cell ratio values are 0.70 or higher in 3D static culture. This high discrepancy between Type B cells and Type A cells'  $\alpha^*$  was the first alarmed evidence of the different state of Type B cells. As quoted before<sup>48,112</sup>, one reason for this might have to do with the increase of the shear stress caused by the continuous agitation in the bioreactor, compared



to the dimple plate, in which there is none. Even if manageable until a certain level, the shear forces still bring damage to the cells, which in this case could be one of the major factors that influence the cells' adaptation and proliferation.

Then, regarding the apparent specific growth rate, it was expected that the  $\mu^{aPP}$  would overall decrease in the Type B cells, compared to Type A, right after analysing the results from the first 24 hours of culture, even if the ROCK inhibitor was in the culture for a longer time. However, some aspects could be understood by the presented data.

The first one was that the highest value obtained for the  $\mu^{aPP}$  was in static culture, with the presence of the ROCK inhibitor in the culture for 96 hours. One reason for the high value in this case has to do with what was quoted previously<sup>57</sup>. Even though different strains of hiPSC were used in this reference, it was concluded that 3D dynamic culture, compared to 3D static culture, resulted in higher shear stress that leads to the disruption of the cell-synthesized ECM, directly suppressing the activation of the cadherin-catenin signalling. This idea could be reinforced by checking the similarity of values in the 3D static culture with the ROCK inhibitor present for 48 hours, since the values of  $2.84 \times 10^{-2} \text{ h}^{-1}$  has a discrepancy of only about 5.56% from the value of  $3.00 \times 10^{-2} \text{ h}^{-1}$ .

Then, when comparing with the Type A cells' value of  $2.30 \times 10^{-2} \text{ h}^{-1}$  with Type B cells' one of  $3.22 \times 10^{-2} \text{ h}^{-1}$ , the latter is clearly higher than previously expected. This means that the number of passages of these cells or even the age of the donor might have affected their adaptation to a different vessel, but also proved to have the capacity of making a great recuperation with the progression of the culture time. Moreover, in static environment, it was shown before that the ECM accumulates at the periphery of the aggregates as time goes by. This difference in the distribution of the ECM could have happened in Type B cells, so their growth under dynamic conditions suggested that mechanical stress induced by the liquid flow was prevented because of the ECM covering the surface of the aggregates<sup>57,113</sup>.

Surprisingly, the time length of ROCK inhibitor in culture barely changed the result in 3D dynamic culture, although it largely contributed to a higher value in 3D static culture. The 96 hours exposure of ROCK inhibitor showed to have increased the  $\mu^{aPP}$  value from  $2.84 \times 10^{-2} \text{ h}^{-1}$  to  $3.57 \times 10^{-2} \text{ h}^{-1}$ , an increase much more considerable than in dynamic culture, in which the values were very similar, of  $3.22 \times 10^{-2} \text{ h}^{-1}$  and  $3.14 \times 10^{-2} \text{ h}^{-1}$ , with the ROCK inhibitor in the culture for 48 hours and 96 hours, respectively. This might be due to the way ECM is developed in both cultures. In the dynamic one, the effect of the mechanical stress from the fluid flow might have prevailed over the effect of ROCK inhibitor in these cells, hence the existence of no difference between the  $\mu^{aPP}$  values. Also, and obviously, the physical stress is much more residual in static culture, which might explain the greater contribution of the ROCK inhibitor when in culture for a longer time.

### 4.3.3. Aggregates' Morphology

Images were taken at  $t = 24$  h and  $t = 96$  h, using phase contrast microscopy, and medium was changed at  $t = 48$  h and  $t = 72$  h. The culture's physical characteristics such as turbidity, colour and the presence of any contamination, derived from bacteria or fungus, were also taken into account when analysing the data. At a seeding concentration of  $1.00 \times 10^5$  cells/mL, the cells grew in both the dimples plates and the bioreactors, and the formation of aggregates in both cases was observable after 24 hours.

Examples of the images captured using the phase contrast microscopy for the dimple plates can be observed in Figure 16A-D.

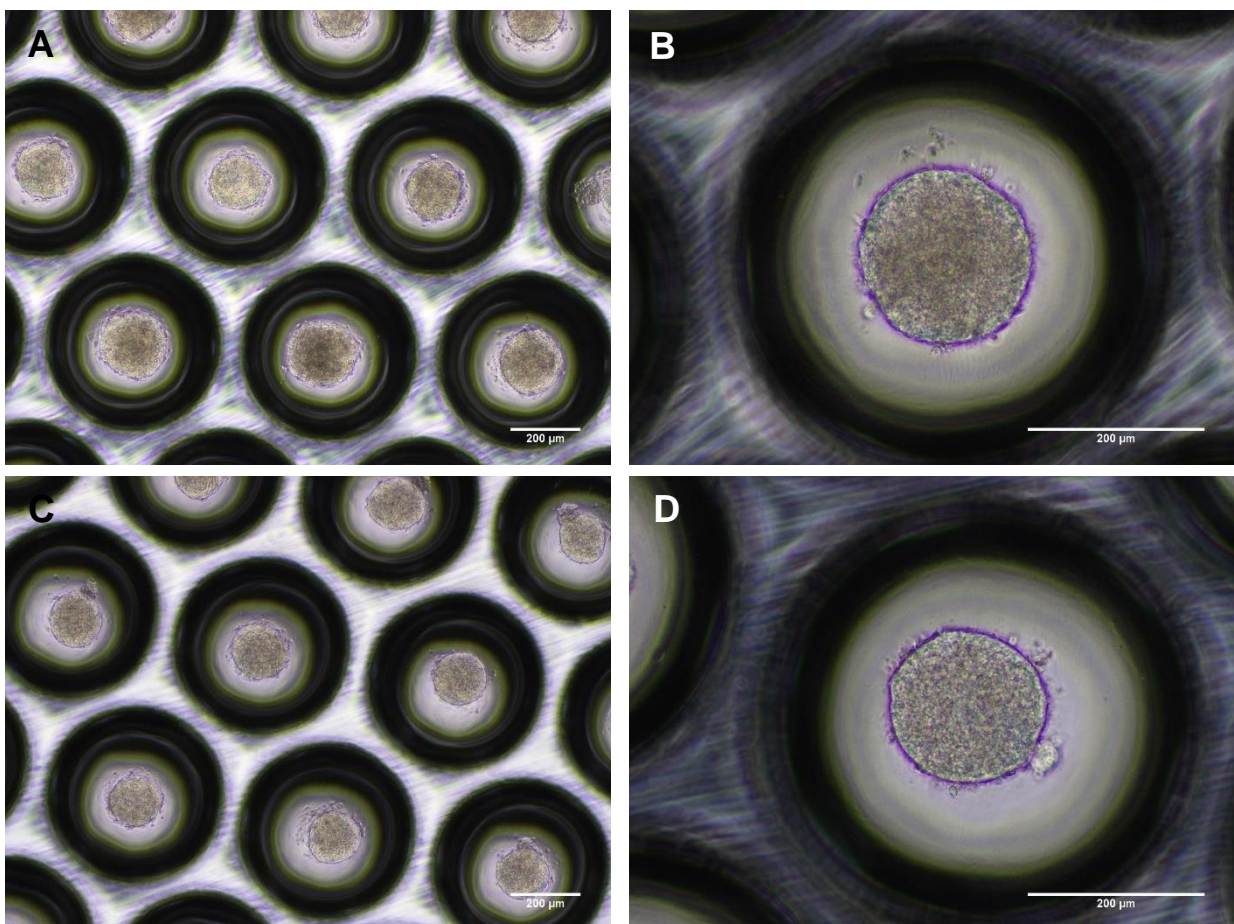


**Figure 16 - Phase contrast microscope images of aggregates composed of Type B cells in the dimple plate.** These images were taken at  $t = 96$  h, with the ROCK inhibitor present in the culture for 48 hours in (A) and (B) and for 96 hours in (C) and (D) ( $n = 1$ ). (Scale bars =  $200 \mu\text{m}$ ).

Cells from this line generally form round aggregates, especially in static culture, with a smooth surface throughout the entire culture time, increasing the aggregate size considerably until the end of the culture time, as shown before and as shown in Annex V, for Type A cells.

After 96 hours, images were captured once more, from samples taken from the dimple plates and the bioreactors, having the ROCK inhibitor in culture for 48 hours and 96 hours, as shown in Figures 17.

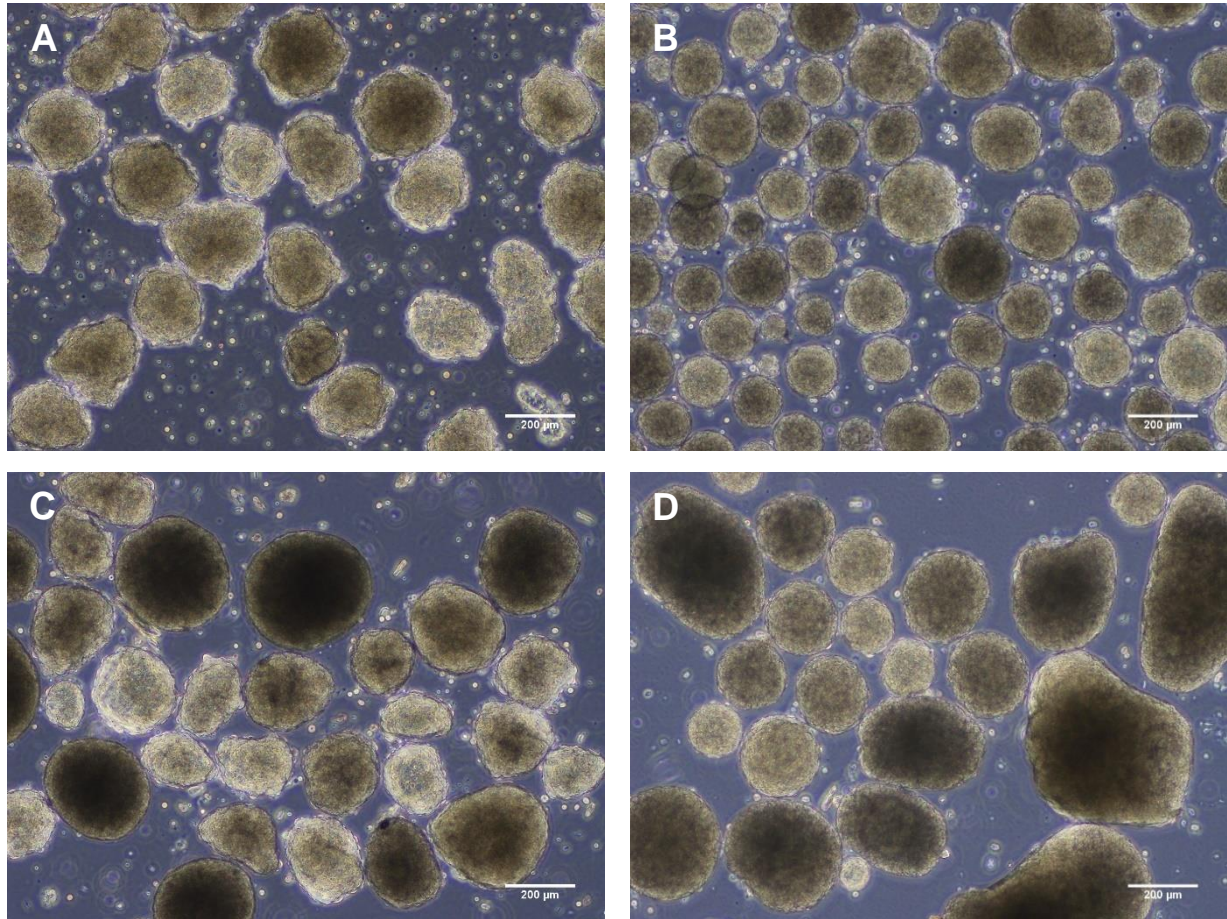


**Figure 17 – Phase contrast microscope images of aggregates composed of Type B cells from the culture 3D static culture, in dimple plates, and 3D dynamic culture, in 30 mL bioreactors.** These images were taken at  $t = 96$  h, showing the aggregates obtained from 3D static culture, with the ROCK inhibitor present in the culture for **(A)** 48 hours and **(B)** 96 hours, and obtained from 3D dynamic culture, with the ROCK inhibitor present in the culture also for **(C)** 48 hours and **(D)** 96 hours ( $n = 1$ ). (Scale bars = 200  $\mu\text{m}$ ).

In the images from Figures 17A-D not only is possible to observe the clear difference between the two type of vessels, but also how the ROCK inhibitor influenced the cultures. With these results, three aspects can be taken into account solemnly from observing the images.

The first one has to do with the evident discrepancy in size between the two types of vessels. Regardless of the exposure time of the cells to the ROCK inhibitor, the aggregate size was found to be larger in dynamic conditions than in static conditions. This was expected, since it has been previously stated that the dynamic environment, such as from bioreactors, might be the answer for the scaling-up process in regards to future applications that require a large number of cells.

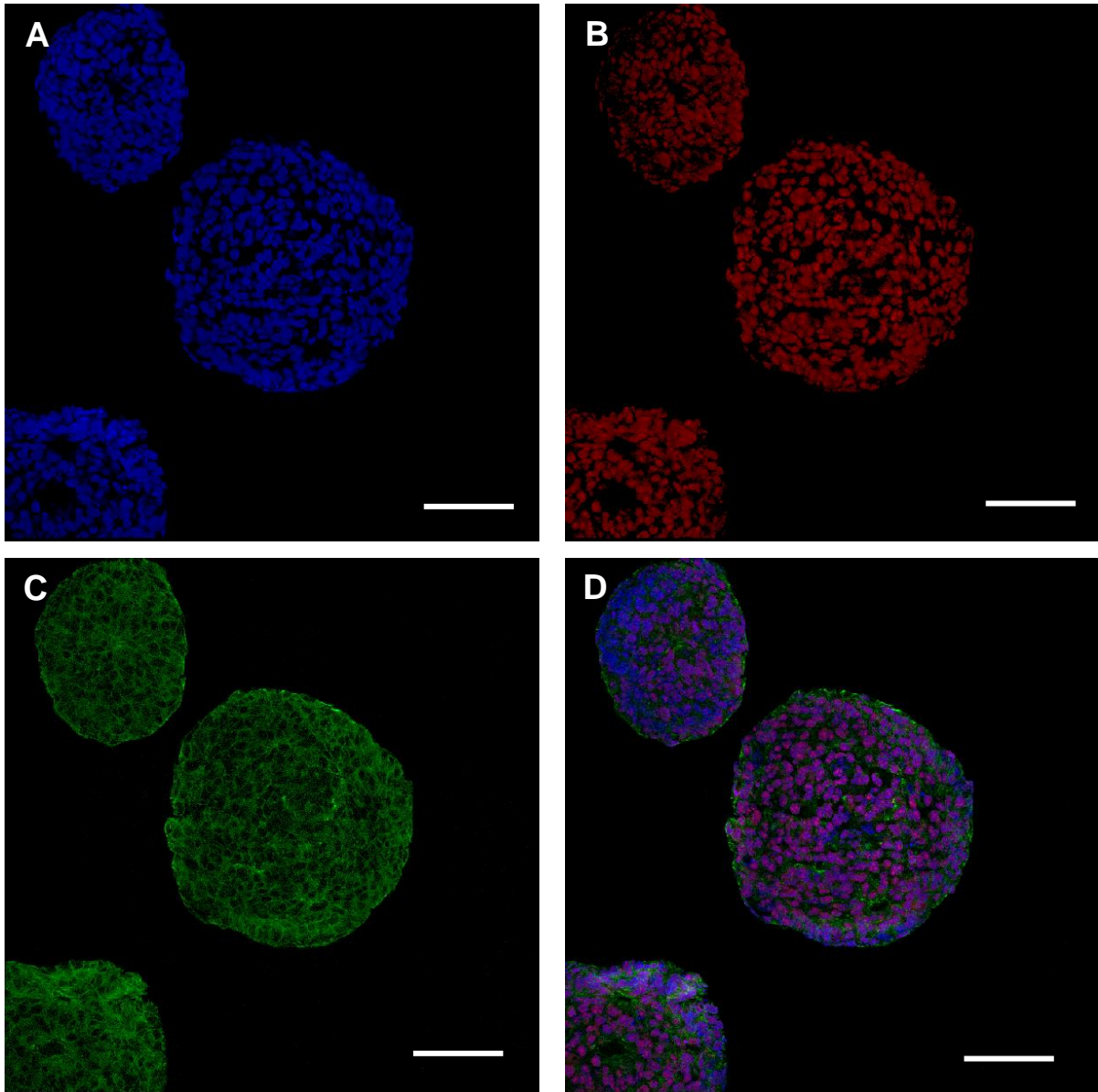
Another aspect that is possible to observe after determining the aggregates' diameter after 96 hours (Figure 15), was that time exposure to ROCK inhibitor for both 48 and 96 hours did not affect the size of the aggregates in the case of the dimple plates, although the difference was more noticeable in the case of the bioreactors, as previously stated.

Finally, the permanency of the ROCK inhibitor in the culture might have influenced the shape of the aggregates. It is notorious that the aggregates with higher exposure to the ROCK inhibitor presented a more regular spherical shape and smooth surface, when compared to the 48 hours exposure in both dynamic and static conditions. The same morphological characteristics can also be observed in Type A cells, even if the exposure to the ROCK inhibitor was longer (Annex V). The ROCK inhibitor is known to play a crucial role on the cytoskeleton of the cells, remodelling it and affecting the actomyosin contractility which is easily affected by the ECM disruption induced by the shear forces of the dynamic flow, hence the change in the aggregates' morphology<sup>114</sup>.

Lastly, it was applied an immunostaining technique in order to generally understand how the aggregate size influenced the quality of the cells.

Subsequently to harvesting, counting and capturing images using phase contrast and bright-field microscopy, the cells were frozen using liquid nitrogen and kept at -80°C for later immunostaining. After meticulously sectioning several samples of aggregates obtained with a thickness of 10 µm, an immunohistological analysis was performed in order to elucidate about the state of development of the cells in the aggregates, especially regarding their size.

The aggregates used to understand these characteristics were collected from the 30 mL bioreactor, with the ROCK inhibitor for 48 hours and culture time of 96 hours. The markers used targeted Ki-67, a proliferation marker, and E-cadherin, a cell-cell adhesion molecule. DAPI counterstaining was also used to detect the cells' nuclei. Figures 18A-D and 19A-D show the expression of these three markers in two examples of aggregates, in which is visible the variation of expression depending on the diameter of the aggregates.



**Figures 18 - Immunostaining images of Type B cells, cultured in a 30 mL bioreactor operating for 96 hours, with the ROCK inhibitor in the culture for 48 hours. The images represent the expression of (A) DAPI, (B) Ki-67, (C) E-cadherin and (D) the merge of the three late results (n = 1). (Scale bars = 100  $\mu$ m).**

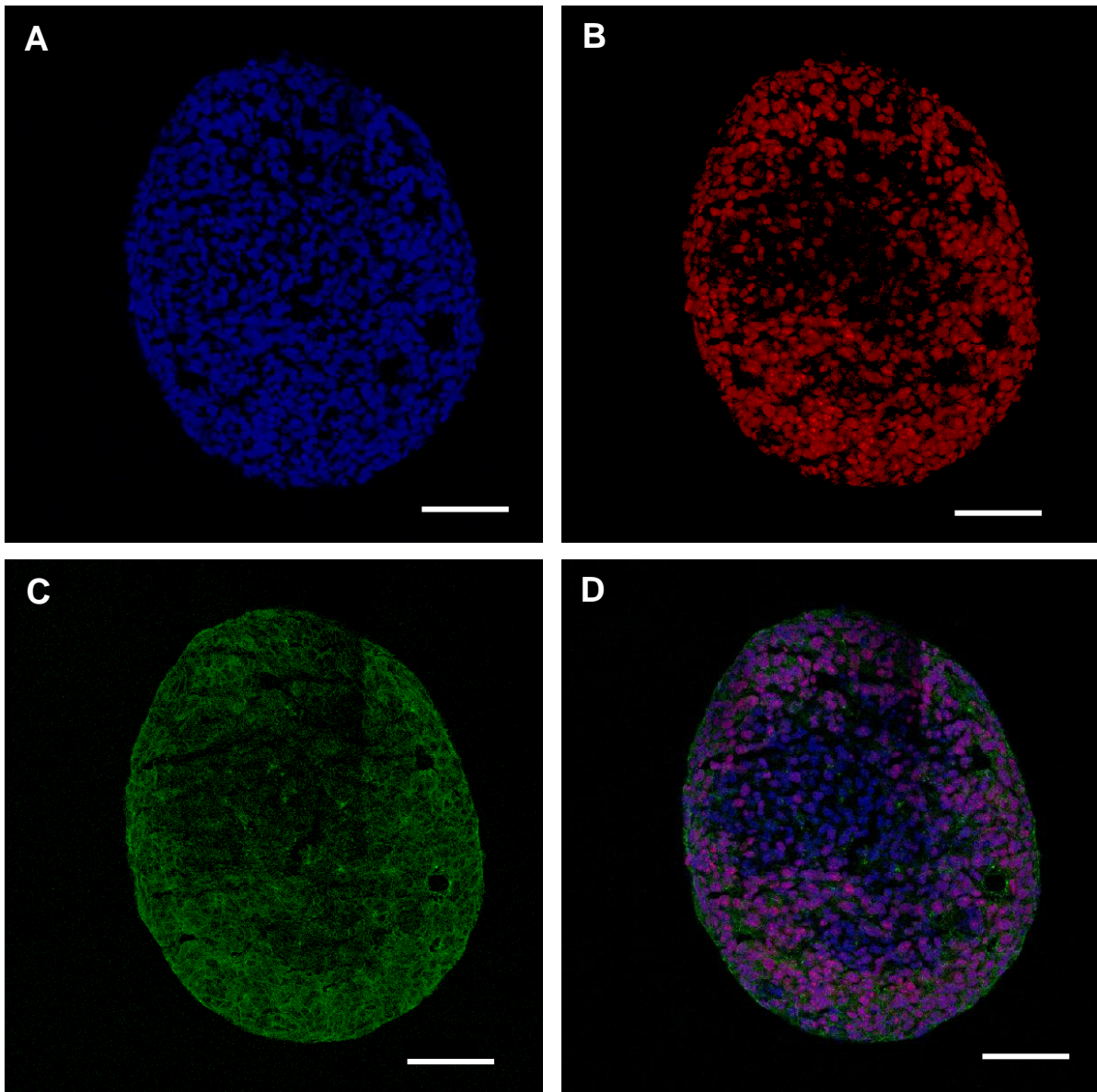


**Figure 19 - Immunostaining images of Type B cells, cultured in a 30 mL bioreactor operating for 96 hours, with the ROCK inhibitor in the culture for 48 hours.** The images represent the expression of **(A)** DAPI, **(B)** Ki-67, **(C)** E-cadherin and **(D)** the merge of the three late results (n = 1). (Scale bars = 100  $\mu$ m).

From the previous immunostaining results obtained, it is possible to observe the expression of DAPI homogeneously in both aggregates' sections, in Figure 18A-D and 19A-D, staining the cells' nuclei.

The protein Ki-67 is strongly associated with cell proliferation, so it works as an excellent culture growth marker.<sup>115</sup> As it can be seen in Figure 18B, in smaller aggregates, the expression of Ki-67 is mainly homogenous in all cells of the aggregate's section. However, in a larger aggregate such as the one from Figure 19B, the centre of the aggregate showed lower expression levels. This suggests that cells in the centre might have started entering the stationary phase of growth sooner than cells on the

periphery, due to the reduction of diffusion of components essential for the proliferation of the cells from the medium to the centre of the aggregates. This quiescence state would later lead to the triggering of apoptosis mechanisms, showed by the low or non-existent the expression of Ki-67 in the centre of the aggregates, comparing to the cells in the periphery<sup>106</sup>.

As for the E-cadherin, this is a protein that mediates cell-cell cohesion, playing an important role in the cells' survival and self-renewal, which can also be used as an undifferentiation indicator since it is able to tie to the transcription factor circuit that triggers the transcription factor OCT4, a widely used pluripotency marker<sup>116</sup>.

By analysing the E-cadherin expression, it is possible to state that the aggregates' size also influences its expression, since the one with smaller diameter, the E-cadherin expression is uniformly distributed in the periphery of the cells (Figure 18C), but the same is not true for aggregate in Figures 19C. As central necrosis expanded, the excretion of ECM components would consequently decrease, resulting in a lower protein expression in the immunostaining results<sup>106,117</sup>. Even so, it is relevant to add that aggregates too small might also result in cell apoptosis due to the low cell-cell contact mediated by E-cadherin, leading to a lower survival rate.

In conclusion, the larger the aggregates, typical from dynamic cultures, the lower is the diffusion rate of components into the middle of the aggregates, leading to the death of the cells in that area. The immunostaining results permitted to conclude that aggregates composed of Type B cells have a Ki-67 and E-cadherin expression similar to other lines of hiPSCs from the literature, according to the size of the aggregate.

Furthermore, even if the highest result obtained for the apparent specific growth rate was in 3D static culture, the obtained aggregates had an overall lower diameter when compared to the dynamic cultures. Due to this, the static culture's aggregates could possibly have generated more uniform aggregates in terms of number of cells in an active phase of development, such as mitosis. Probably, if the culture time proceeded for more than 96 hours, the maintenance of the viability of the cells would have been seriously compromised, leading to a decrease in the proliferation rate of the cells and consequently to a drop in the apparent specific growth rate value, due to the inhibitory competition for the resources in the culture.

Finally, it was possible to conclude from the results in this thesis that the cells from stock B might have undergone modifications at genetical level due to several aspects.

One of them, might be related to the number of passages the Type B culture was subjected to. According to the information provided by the laboratory, Type A culture has suffered not more than 30 passages, while in the case of the stock for Type B cells the number was at least 65 passages. Cells that were kept for a long time and thus suffered several passages might have begun changing their physiological and morphological proprieties, resulting in differences in their karyotype that affected their phenotype subsequently, when compared to Type A cells, from the same line, as previously tested out.

Even so, this should not be a reason for the difference in characteristics of both groups, since pluripotent stem cells are known for having unlimited capacity for self-renewal, while maintaining their

pluripotency. The hypothesis falls on the fact that the maintenance protocol might have not have been followed truthfully and equally every passaging time. Since these cells are extremely sensitive to changes in culture conditions and handling techniques, this fact might have resulted in modifications in Type B cells at the genome level.

Also, and as commented before, the age of the donor is an important factor when it comes to the quality of the cells, since it influences the activity and expression of proteins that regulate the cellular pathways under stress conditions. However, in this case, this factor is unknown and therefore impossible to discuss.



# 5. CONCLUSIONS AND FUTURE PERSPECTIVES

Human induced pluripotent stem cells have shown to have clinical potential due to their self-renewal characteristics, capable of taking cell therapies to a new level. The fact that hiPSCs have the advantage of few incompatibility problems with the patient and also overcome some ethical issues that hESCs do not, is highly motivating to continue the research on these cells. Even so, the design of robust culture systems that would allow the scaling-up process with guaranteed reproducibility is still a topic under constant study.

In this thesis, the two stocks from hiPSCs, both from the 1383D2 line, were compared, since one of them have suffered transformations that affected the phenotype of the cells. These altered cells, named Type B cells, were studied and compared to other stock with cells from the same line, named Type A cells, in order to take conclusions about the viability of Type B cells in future works.

Even if with these outcomes, the fact that some of the results are not completely comparable or statistically relevant due to the lack of replicates of certain experiments, mainly due to time restraints, is still an aspect to be noted. Nevertheless, and taking into account the unexpected turn that this work came across initially, it was imperative for a laboratory specialised in the standardization of the processes regarding stem cells technology to understand the differences found in the stocks from the same line of cells. Comparing the exposure time of the cells to the ROCK inhibitor and the 2D with the 3D culture environment, and the static with dynamic conditions, the shear stress was believed to be one of the most crucial factors that would affect the adaptation and further growth of Type B cells. Albeit these cells clearly presented modifications in regards to Type A cells, which were exactly from the same line, the high apparent specific growth rate proved to be a game-changer. Even if with low live cell ratios, Type B cells were able to proliferate more than Type A culture. This is a very motivating reason to use these cells in the future for other experiments, even though further research at genetical level must be done in order to proceed with their research. Moreover, the immunostaining results reinforced the idea that Type B cells are, in fact, prone to be viable to be used in upcoming research works, since their behaviour was expectable when compared to the literature.

Overall, this work consisted of a first approach to the understanding of the behaviour, quality, morphology and other aspects of these altered cells. As future work, it would be of interest to test how other culture parameters might affect the development of these cells, such as the initial cell density, the concentration of ROCK inhibitor in the culture or the agitation speed, in the case of the bioreactor. Furthermore, testing pluripotency markers such as OCT4, NANOG or SOX2 would support the conclusions taken about the undifferentiated state of these cells. This work would include testing these markers and also the Ki-67 and the E-cadherin ones for aggregates grown in 3D static culture and possibly also in 2D culture.

As later work, certainly that a genome sequencing technique to both types of cells must be considered. Firstly, because it would show the variations that could have happened in the karyotype of Type B cells in regards of Type A cells and conclude if Type B cells are, in fact, safe to be used in future applications. If their karyotype showed to be within the approved standards from stem cell research, then these cells might lead to new and promising outcomes in future works. Moreover, this analysis could also finally help to elucidate which genes were affected that could have explained the change in phenotype and proliferation rate.

In conclusion, this area of study embraces many features that must be carefully taken into account, so there is still further work to be done to wholly optimize the process of production of these cultures at a larger scale. The previous and still on-going investigations have brought encouraging results to continue the exploration in this branch of bioengineering, medicine and computer science, which, with truthful interest from the right institutions, will undoubtedly lead to a ground-breaking impact in the field.

# REFERENCES

1. Tabansky, I. & Stern, J. N. H. Stem Cells in Neuroendocrinology. 11–24 (2016). doi:10.1007/978-3-319-41603-8
2. Zomer, H. D., Vidane, A. S., Gonçalves, N. N. & Ambrosio, C. E. Mesenchymal and induced pluripotent stem cells : general insights and clinical perspectives. *Stem Cells Cloning Adv. Appl.* **8**, 125–134 (2015).
3. A. Giordano, U. G. and I. M. From the Laboratory Bench to the Patient's Bedside: An Update on Clinical Trials With Mesenchymal Stem Cells. *J. Cell. Physiol.* **207**, 12–22 (2007).
4. Thomson, J. A. Embryonic Stem Cell Lines Derived from Human Blastocysts. *Science (80- )*. **282**, 1145–1147 (1998).
5. Winslow, T. Regenerative Medicine 2006 © 2006. (2006).
6. Evans, M. J. & Kaufman, M. H. Establishment in culture of pluripotential cells from mouse embryos. *Nature* **292**, 154–156 (1981).
7. Martin, G. R. Isolation of a pluripotent cell line from early mouse embryos cultured in medium conditioned by teratocarcinoma stem cells. *Proc. Natl. Acad. Sci.* **78**, 7634–7638 (1981).
8. Chambers, I. & Smith, A. Self-renewal of teratocarcinoma and embryonic stem cells. *Oncogene* **23**, 7150–7160 (2004).
9. Cooke, M. J., Stojkovic, M. & Przyborski, S. A. Growth of Teratomas Derived from Human Pluripotent Stem Cells Is Influenced by the Graft Site. *Stem Cells Dev.* **15**, 254–259 (2006).
10. Hentze, H. *et al.* Teratoma formation by human embryonic stem cells: Evaluation of essential parameters for future safety studies. *Stem Cell Res.* **2**, 198–210 (2009).
11. Lo, B. & Parham, L. Ethical issues in stem cell research. *Endocr. Rev.* **30**, 204–213 (2009).
12. Yamanaka, S. A Fresh Look at iPS Cells. *Cell* **137**, 13–17 (2009).
13. Liang, G. & Zhang, Y. Embryonic stem cell and induced pluripotent stem cell: An epigenetic perspective. *Cell Res.* **23**, 49–69 (2013).
14. Buganim, Y., Faddah, D. A. & Jaenisch, R. Mechanisms and models of somatic cell reprogramming. *Nat. Rev. Genet.* **14**, 427–439 (2013).
15. Kole, D., Ambady, S., Page, R. L. & Dominko, T. Maintenance of Multipotency in Human Dermal Fibroblasts Treated with *Xenopus laevis* Egg Extract Requires Exogenous Fibroblast Growth Factor-2. *Cell. Reprogram.* **16**, 18–28 (2014).
16. Giorgetti, A. *et al.* Generation of Induced Pluripotent Stem Cells from Human Cord Blood Using OCT4 and SOX2. *Cell Stem Cell* **5**, 353–357 (2009).
17. Loh, Y.-H. *et al.* Generation of induced pluripotent stem cells from human blood. *Blood* **113**,

- 5476–5479 (2009).
18. Hui, H. *et al.* Stem Cells : General Features and Characteristics. *Stem Cells Clin. Res.* 1–20 (2011). doi:10.5772/740
  19. Zacharias, D. G., Nelson, T. J., Mueller, P. S. & Hook, C. C. The science and ethics of induced pluripotency: What will become of embryonic stem cells? *Mayo Clin. Proc.* **86**, 634–640 (2011).
  20. Kang, S. *et al.* Characteristic analyses of a neural differentiation model from iPSC-derived neuron according to morphology, physiology, and global gene expression pattern. *Sci. Rep.* **7**, 1–11 (2017).
  21. Belmonte, J. C. I., Ellis, J., Hochedlinger, K. & Yamanaka, S. Induced pluripotent stem cells and reprogramming: Seeing the science through the hype. *Nat. Rev. Genet.* **10**, 878–883 (2009).
  22. Lo Sardo, V. *et al.* Influence of donor age on induced pluripotent stem cells. *Nat. Biotechnol.* **35**, 69–74 (2017).
  23. Schulz, T. C. *et al.* A scalable system for production of functional pancreatic progenitors from human embryonic stem cells. *PLoS One* **7**, (2012).
  24. Kushner, J. A., MacDonald, P. E. & Atkinson, M. A. Stem cells to insulin secreting cells: Two steps forward and now a time to pause? *Cell Stem Cell* **15**, 535–536 (2014).
  25. Schwartz, S. D. *et al.* Human embryonic stem cell-derived retinal pigment epithelium in patients with age-related macular degeneration and Stargardt's macular dystrophy: Follow-up of two open-label phase 1/2 studies. *Lancet* **385**, 509–516 (2015).
  26. Cyranoski, D. (2014). Japanese woman is first recipient of next-generation stem cells. Nature News (Nature Publishing Group), September 12, 2014. <http://www.nature.com/news/japanese-woman-is-first-recipient-of-nextgeneration-stem-cells-1.15915>.
  27. Howard, D., Buttery, L. D., Shakesheff, K. M. & Roberts, S. J. Tissue engineering: Strategies, stem cells and scaffolds. *J. Anat.* **213**, 66–72 (2008).
  28. Uchida, H. *et al.* A xenogeneic-free system generating functional human gut organoids from pluripotent stem cells. *JCI Insight* **2**, 1–13 (2017).
  29. Shiba, Y. *et al.* Allogeneic transplantation of iPS cell-derived cardiomyocytes regenerates primate hearts. *Nature* **538**, 388–391 (2016).
  30. Piao, J. *et al.* Human embryonic stem cell-derived oligodendrocyte progenitors remyelinate the brain and rescue behavioral deficits following radiation. *Cell Stem Cell* **16**, 198–210 (2015).
  31. Grskovic, M., Javaherian, A., Strulovici, B. & Daley, G. Q. Induced pluripotent stem cells: opportunities for disease modelling and drug discovery. *Nat. Rev. Drug Discov.* **10**, 915–929 (2011).
  32. Zuba-surma, E. K., Wojakowski, W., Madeja, Z. & Ratajczak, M. Z. Stem Cells as a Novel Tool for Drug Screening and Treatment of Degenerative Diseases. 2644–2656 (2012).

33. Saul J. Sharkis, Richard J. Jones, Curt Civin, and Y.-Y. J. Pluripotent Stem Cell–Based Cancer Therapy: Promise and Challenges. *Nano* **6**, 2166–2171 (2012).
34. Trounson, A. & DeWitt, N. D. Pluripotent stem cells progressing to the clinic. *Nat. Rev. Mol. Cell Biol.* **17**, 194–200 (2016).
35. European Medicines Agency. Guideline on human cell-based medicinal products. *EMA EMA*, EMEA/CHMP/410869/2006 (2008).
36. FDA. Guidance for Industry: Regulation of Human Cells, Tissues, and Cellular and Tissue-Based Products (HCT/PS) Small Entity Compliance Guide. *Small Entity Compliance Guid.* (2007).
37. Unger, C., Skottman, H., Blomberg, P., Sirac dilber, M. & Hovatta, O. Good manufacturing practice and clinical-grade human embryonic stem cell lines. *Hum. Mol. Genet.* **17**, 48–53 (2008).
38. Nakagawa, M. *et al.* A novel efficient feeder-free culture system for the derivation of human induced pluripotent stem cells. *Sci. Rep.* **4**, 1–7 (2014).
39. Eiselleova, L. *et al.* Comparative study of mouse and human feeder cells for human embryonic stem cells. *Int. J. Dev. Biol.* **52**, 353–363 (2008).
40. Takahashi, K. & Yamanaka, S. Supplemental Data Induction of Pluripotent Stem Cells from Mouse Embryonic and Adult Fibroblast Cultures by Defined Factors. *Reactions* **126**, 663–676 (2006).
41. Llames, S., García-Pérez, E., Meana, Á., Larcher, F. & del Río, M. Feeder Layer Cell Actions and Applications. *Tissue Eng. Part B Rev.* **21**, 345–353 (2015).
42. Matsuda, Y., Takahashi, K., Kamioka, H. & Naruse, K. Human gingival fibroblast feeder cells promote maturation of induced pluripotent stem cells into cardiomyocytes. *Biochem. Biophys. Res. Commun.* 1–7 (2018). doi:10.1016/j.bbrc.2018.07.116
43. Christian Unger Ulrika Felldin Agneta Nordenskjöld M. Sirac Dilber Outi Hovatta. Derivation of Human Skin Fibroblast Lines for Feeder Cells of Human Embryonic Stem Cells. (2008).
44. Xu, C. *et al.* Feeder-free growth of undifferentiated human embryonic stem cells. *Nat. Biotechnol.* **19**, 971–974 (2001).
45. Park, S. & Mostoslavsky, G. Generation of Human Induced Pluripotent Stem Cells Using a Defined, Feeder-Free Reprogramming System. *Curr. Protoc. Stem Cell Biol.* **45**, 1–15 (2018).
46. Chen, K. G., Mallon, B. S., McKay, R. D. G. & Robey, P. G. Human pluripotent stem cell culture: Considerations for maintenance, expansion, and therapeutics. *Cell Stem Cell* **14**, 13–26 (2014).
47. Ludwig, T. E. *et al.* Derivation of human embryonic stem cells in defined conditions. *Nat. Biotechnol.* **24**, 185–187 (2006).
48. Wang, Y. *et al.* Scalable expansion of human induced pluripotent stem cells in the defined xeno-free E8 medium under adherent and suspension culture conditions. *Stem Cell Res.* **11**, 1103–1116 (2013).

49. Chen, G. *et al.* Chemically defined conditions for human iPSC derivation and culture. *Nat. Methods* **8**, 424–429 (2011).
50. Squillaro, T., Peluso, G. & Galderisi, U. Review Clinical Trials With Mesenchymal Stem Cells : An Update. **25**, 829–848 (2016).
51. Macreadie, I. Cell banking and mutation.
52. Crook, J. M., Hei, D. & Stacey, G. The international stem cell banking initiative (ISCBI): Raising standards to bank on. *Vitr. Cell. Dev. Biol. - Anim.* **46**, 169–172 (2010).
53. Abbasalizadeh, S. & Baharvand, H. Technological progress and challenges towards cGMP manufacturing of human pluripotent stem cells based therapeutic products for allogeneic and autologous cell therapies. *Biotechnol. Adv.* **31**, 1600–1623 (2013).
54. Shan, X., Roberts, C., Lan, Y. & Percec, I. Age Alters Chromatin Structure and Expression of SUMO Proteins under Stress Conditions in Human Adipose-Derived Stem Cells. *Sci. Rep.* **8**, 11502 (2018).
55. Konagaya, S., Ando, T., Yamauchi, T., Suemori, H. & Iwata, H. Long-term maintenance of human induced pluripotent stem cells by automated cell culture system. *Sci. Rep.* **5**, 1–9 (2015).
56. Beers, J. *et al.* Passaging and colony expansion of human pluripotent stem cells by enzyme-free dissociation in chemically defined culture conditions. *Nat. Protoc.* **7**, 2029–2040 (2012).
57. Kato, Y., Kim, M. H. & Kino-oka, M. Comparison of growth kinetics between static and dynamic cultures of human induced pluripotent stem cells. *J. Biosci. Bioeng.* **xx**, 1–5 (2018).
58. Bock, C. *et al.* Reference maps of human es and ips cell variation enable high-throughput characterization of pluripotent cell lines. *Cell* **144**, 439–452 (2011).
59. Watanabe, K. *et al.* A ROCK inhibitor permits survival of dissociated human embryonic stem cells. *Nat. Biotechnol.* **25**, 681–686 (2007).
60. Zhang, K. & Chen, J. F. The regulation of integrin function by divalent cations. *Cell Adhes. Migr.* **6**, 20–29 (2012).
61. Naonori, I., Masafumi, K., Naohito, O. & Kazuki, M. Rho kinase inhibitors. **50**, 143 (2007).
62. Hu, E. & Lee, D. Rho kinase as potential therapeutic target for cardiovascular diseases: opportunities and challenges. *Expert Opin Ther Targets* **9**, 715–736 (2005).
63. Quintin, S., Gally, C. & Labouesse, M. Epithelial morphogenesis in embryos: asymmetries, motors and brakes. *Trends Genet.* **24**, 221–230 (2008).
64. Chen, G., Hou, Z., Gulbranson, D. R. & Thomson, J. A. Actin-myosin contractility is responsible for the reduced viability of dissociated human embryonic stem cells. *Cell Stem Cell* **7**, 240–248 (2010).
65. Okeyo, K. O., Adachi, T., Sunaga, J. & Hojo, M. Actomyosin contractility spatiotemporally regulates actin network dynamics in migrating cells. *J. Biomech.* **42**, 2540–2548 (2009).

66. Ohgushi, M. *et al.* Molecular pathway and cell state responsible for dissociation-induced apoptosis in human pluripotent stem cells. *Cell Stem Cell* **7**, 225–239 (2010).
67. Lavon, N., Zimerman, M. & Itskovitz-Eldor, J. Scalable Expansion of Pluripotent Stem Cells. *Adv. Biochem. Eng. Biotechnol.* **123**, 127–141 (2017).
68. Kamao, H. *et al.* Characterization of human induced pluripotent stem cell-derived retinal pigment epithelium cell sheets aiming for clinical application. *Stem Cell Reports* **2**, 205–218 (2014).
69. Silva, C. A. M. L. Bioreactors for Stem Cell Manufacturing. Available at: [https://fenix.tecnico.ulisboa.pt/downloadFile/1407993358860442/Class17\\_14Nov.pdf](https://fenix.tecnico.ulisboa.pt/downloadFile/1407993358860442/Class17_14Nov.pdf).
70. Want, A. J., Nienow, A. W., Hewitt, C. J. & Coopman, K. Large-scale expansion and exploitation of pluripotent stem cells for regenerative medicine purposes: beyond the T flask. *Regen. Med.* **7**, 71–84 (2012).
71. Fridley, K. M., Fernandez, I., Li, M.-T. A., Kettlewell, R. B. & Roy, K. Unique differentiation profile of mouse embryonic stem cells in rotary and stirred tank bioreactors. *Tissue Eng. Part A* **16**, 3285–98 (2010).
72. Rodrigues, C. A. V, Fernandes, T. G., Diogo, M. M., da Silva, C. L. & Cabral, J. M. S. Stem cell cultivation in bioreactors. *Biotechnol. Adv.* **29**, 815–829 (2011).
73. Correia, C. *et al.* Combining Hypoxia and Bioreactor Hydrodynamics Boosts Induced Pluripotent Stem Cell Differentiation Towards Cardiomyocytes. *Stem Cell Rev. Reports* **10**, 786–801 (2014).
74. Pankaj Godara, C. D. M. and R. E. N. Design of bioreactors for mesenchymal stem cell tissue engineering. *J. Chem. Technol. Biotechnol.* **83**, 408–420 (2008).
75. Serra, M., Brito, C., Correia, C. & Alves, P. M. Process engineering of human pluripotent stem cells for clinical application. *Trends Biotechnol.* **30**, 350–359 (2012).
76. Oh, S. K. W. *et al.* Long-term microcarrier suspension cultures of human embryonic stem cells. *Stem Cell Res.* **2**, 219–230 (2009).
77. Gupta, P. *et al.* Optimization of agitation speed in spinner flask for microcarrier structural integrity and expansion of induced pluripotent stem cells. *Cytotechnology* **68**, 45–59 (2016).
78. Bardy, J. *et al.* Microcarrier Suspension Cultures for High-Density Expansion and Differentiation of Human Pluripotent Stem Cells to Neural Progenitor Cells. *Tissue Eng. Part C Methods* **19**, 166–180 (2013).
79. Fernandes, A. M. *et al.* Mouse embryonic stem cell expansion in a microcarrier-based stirred culture system. *J. Biotechnol.* **132**, 227–236 (2007).
80. Chen, A. K. L., Chen, X., Choo, A. B. H., Reuveny, S. & Oh, S. K. W. Critical microcarrier properties affecting the expansion of undifferentiated human embryonic stem cells. *Stem Cell Res.* **7**, 97–111 (2011).
81. Kehoe, D. E., Jing, D., Lock, L. T. & Tzanakakis, E. S. Scalable Stirred-Suspension Bioreactor Culture of Human Pluripotent Stem Cells. *Tissue Eng.* **16**, 405–21 (2010).

82. Badenes, S. M., Fernandes, T. G., Rodrigues, C. A. V., Diogo, M. M. & Cabral, J. M. S. Microcarrier-based platforms for in vitro expansion and differentiation of human pluripotent stem cells in bioreactor culture systems. *J. Biotechnol.* **234**, 71–82 (2016).
83. Fernandes-Platzgummer, A., Diogo, M. M., Baptista, R. P., Silva, C. L. da & Cabral, J. M. S. Scale-up of mouse embryonic stem cell expansion in stirred bioreactors. *Biotechnol. Prog.* **27**, 1421–1432 (2011).
84. Fan, Y., Hsiung, M., Cheng, C. & Tzanakakis, E. S. Facile Engineering of Xeno-Free Microcarriers for the Scalable Cultivation of Human Pluripotent Stem Cells in Stirred Suspension. *Tissue Eng. Part A* **20**, 131128071850006 (2013).
85. Sara M. Badenes, Tiago G. Fernandes, C. A. V. R. & Maria Margarida Diogo, and J. M. S. C. Scalable Expansion of Human-Induced Pluripotent Stem Cells in Xeno-Free Microcarriers. *Methods Mol. Biol.* 257–284 (2014). doi:10.1007/7651
86. Sart, S., Agathos, S. N. & Li, Y. Engineering stem cell fate with biochemical and biomechanical properties of microcarriers. *Biotechnol. Prog.* **29**, 1354–1366 (2013).
87. Badenes, S. M. *et al.* Defined essential 8' medium and vitronectin efficiently support scalable xeno-free expansion of human induced pluripotent stem cells in stirred microcarrier culture systems. *PLoS One* **11**, 155296 (2016).
88. Reibetanz, U., H??bner, D., Jung, M., Liebert, U. G. & Claus, C. Influence of Growth Characteristics of Induced Pluripotent Stem Cells on Their Uptake Efficiency for Layer-by-Layer Microcarriers. *ACS Nano* **10**, 6563–6573 (2016).
89. Phillips, B. W. *et al.* Attachment and growth of human embryonic stem cells on microcarriers. *J. Biotechnol.* **138**, 24–32 (2008).
90. Jenkins, M., Bilsland, J., Allsopp, T. E., Ho, S. V. & Farid, S. S. Patient-specific hiPSC bioprocessing for drug screening: Bioprocess economics and optimisation. *Biochem. Eng. J.* **108**, 84–97 (2016).
91. Sart, S., Bejoy, J. & Li, Y. Characterization of 3D pluripotent stem cell aggregates and the impact of their properties on bioprocessing. *Process Biochem.* **59**, 276–288 (2017).
92. Tostões, R. M. *et al.* Human liver cell spheroids in extended perfusion bioreactor culture for repeated-dose drug testing. *Hepatology* **55**, 1227–1236 (2012).
93. Meenal Banerjee, R. R. B. Application of hanging drop technique for stem cell differentiation and cytotoxicity studies. *Springer Sci. Media* **51**, 1–5 (2006).
94. Oyamada, M., Takebe, K., Endo, A., Hara, S. & Oyamada, Y. Connexin expression and gap-junctional intercellular communication in ES cells and iPS cells. *Front. Pharmacol.* **4 JUL**, 1–8 (2013).
95. M.G. Todorova, B. Soria, I. Q. Gap Junctional Intercellular a Non-Differentiated and Maintain Embryonic Stem Cells in Communication Is Required to Proliferative State. *J. Cell. Physiol.* **207**,



- 12–22 (2007).
96. Soncin, F. *et al.* E-cadherin acts as a regulator of transcripts associated with a wide range of cellular processes in mouse embryonic stem cells. *PLoS One* **6**, (2011).
  97. Sart, S., Schneider, Y. J., Li, Y. & Agathos, S. N. Stem cell bioprocess engineering towards cGMP production and clinical applications. *Cytotechnology* **66**, 709–722 (2014).
  98. Park, J. *et al.* Microfabrication-based modulation of embryonic stem cell differentiation. *Lab Chip* **7**, 1018–1028 (2007).
  99. Bauwens, C. L. *et al.* Geometric Control of Cardiomyogenic Induction in Human Pluripotent Stem Cells. *Tissue Eng. Part A* **17**, 1901–1909 (2011).
  100. Hsiao, C. & Palecek, S. P. Microwell Regulation of Pluripotent Stem Cell Self-Renewal and Differentiation. *Bionanoscience* **2**, 266–276 (2012).
  101. Kraehenbuehl, T. P., Langer, R. & Ferreira, L. S. Three-dimensional biomaterials for the study of human pluripotent stem cells. *Nat. Methods* **8**, 731–736 (2011).
  102. Eiraku, M. *et al.* Self-organizing optic-cup morphogenesis in three-dimensional culture. *Nature* **472**, 51–58 (2011).
  103. Miranda, C. C. *et al.* A scale out approach towards neural induction of human induced pluripotent stem cells for neurodevelopmental toxicity studies. *Toxicol. Lett.* **294**, 51–60 (2018).
  104. Ungrin, M. D., Joshi, C., Nica, A., Bauwens, C. & Zandstra, P. W. Reproducible, ultra high-throughput formation of multicellular organization from single cell suspension-derived human embryonic stem cell aggregates. *PLoS One* **3**, (2008).
  105. Choi, Y. Y. *et al.* Controlled-size embryoid body formation in concave microwell arrays. *Biomaterials* **31**, 4296–4303 (2010).
  106. Nath, S. C., Horie, M., Nagamori, E. & Kino-oka, M. Size- and time-dependent growth properties of human induced pluripotent stem cells in the culture of single aggregate. *J. Biosci. Bioeng.* **124**, 469–475 (2017).
  107. Amit, M. *et al.* Dynamic suspension culture for scalable expansion of undifferentiated human pluripotent stem cells. *Nat. Protoc.* **6**, 572–579 (2011).
  108. Fok, E. Y. L. & Zandstra, P. W. Shear-Controlled Single-Step Mouse Embryonic Stem Cell Expansion and Embryoid Body-Based Differentiation. *Stem Cells* **23**, 1333–1342 (2005).
  109. Uda, Y. *et al.* Force via integrins but not E-cadherin decreases Oct3/4 expression in embryonic stem cells. *Biochem. Biophys. Res. Commun.* **415**, 396–400 (2011).
  110. Chowdhury, F. *et al.* Material properties of the cell dictate stress-induced spreading and differentiation in embryonic stemcells. *Nat. Mater.* **9**, 82–88 (2010).
  111. Kempf, H., Andree, B. & Zweigerdt, R. Large-scale production of human pluripotent stem cell derived cardiomyocytes. *Adv. Drug Deliv. Rev.* **96**, 18–30 (2016).

112. Mohd Zin, N. K. *et al.* Induced pluripotent stem cell differentiation under constant shear stress. *IFMBE Proc.* **52**, 7–8 (2015).
113. Sachlos, E. & Auguste, D. T. Embryoid body morphology influences diffusive transport of inductive biochemicals: A strategy for stem cell differentiation. *Biomaterials* **29**, 4471–4480 (2008).
114. Humphrey, J. D., Dufresne, E. R. & Schwartz, M. A. Mechanotransduction and extracellular matrix homeostasis. *Nat. Rev. Mol. Cell Biol.* **15**, 802–812 (2014).
115. Scholzen, T. & Gerdes, J. The Ki-67 protein: From the known and the unknown. *J. Cell. Physiol.* **182**, 311–322 (2000).
116. Li, L., Bennett, S. A. L. & Wang, L. Role of E-cadherin and other cell adhesion molecules in survival and differentiation of human pluripotent stem cells. *Cell Adh. Migr.* **6**, 59–73 (2012).
117. Xu, Y. *et al.* Revealing a core signaling regulatory mechanism for pluripotent stem cell survival and self-renewal by small molecules. *Proc. Natl. Acad. Sci.* **107**, 8129–8134 (2010).

# ANNEXES

## ANNEX I

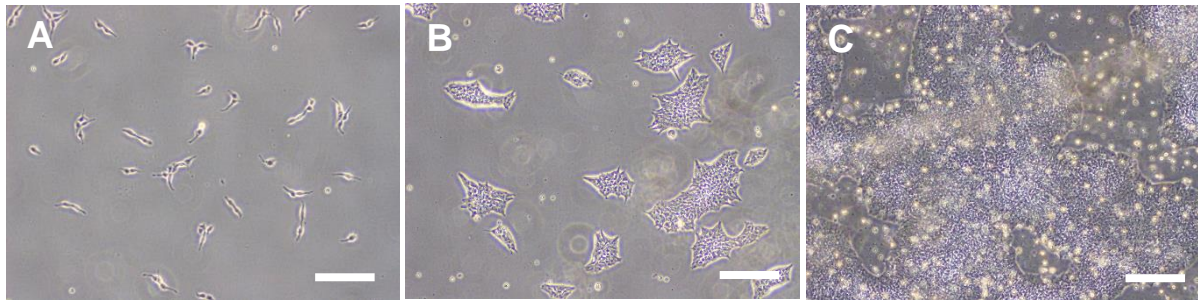


**Figure 20 - Images captured using phase contrast microscope of hiPSC, Type B cells.** Images were taken at **(A)**  $t = 24$  h, **(B)**  $t = 72$  h and **(C)**  $t = 120$  h. Dead cells correspond to the yellow floating spheres. These unpublished results were kindly provided by a laboratory member ( $n = 1$ ). (Scale bars =  $500 \mu\text{m}$ ).

## ANNEX II

**Table 6 – Growth kinetics parameters for the hiPS cells 2D static culture in 8-well plates for Type A cells, for attachment efficiency ( $\alpha$ ) and specific growth rate ( $\mu$ ).** The values represented are the average at  $t = 24$  h and  $t = 120$  h, respectively, for the condition of study of the effect of the ROCK inhibitor in the culture for 24 hours, followed by the standard deviation ( $\pm$ ). These unpublished results were kindly provided by laboratory members ( $n = 1$ ).

	24 h ROCK Inhibitor	
	$\alpha (-)$	$\mu (10^{-2} \text{h}^{-1})$
2D Static Culture	$1.57 \pm 0.05$	$4.91 \pm 0.00$

## ANNEX III

**Table 7 - Results from the Type A cells in 3D dynamic culture for the live cell ratio ( $\alpha^*$ ) and apparent specific growth rate ( $\mu^{app}$ ).** The values represented are the average, followed by the standard deviation ( $\pm$ ), for the culture time of 120 h, for the condition of study of the effect of ROCK inhibitor in the culture for 24 hours and 120 hours. These unpublished results were kindly provided by a laboratory member (n = 1).

	$\alpha^*$ (-)	$\mu^{app}$ ( $10^{-2} \text{ h}^{-1}$ )
24 h ROCKi	0.62 $\pm$ 0.14	2.45 $\pm$ 0.00
120 h ROCKi	0.61 $\pm$ 0.15	3.29 $\pm$ 0.00

## ANNEX IV

**Table 8 - Results from the Type A cells in 3D static culture for the live cell ratio ( $\alpha^*$ ) and apparent specific growth rate ( $\mu^{app}$ ).** The values represented are the average, followed by the standard deviation ( $\pm$ ), for the culture time of 120 h, for the condition of study of the effect of ROCK inhibitor in the culture for 24 hours. These unpublished results were kindly provided by laboratory members (n = 1).

	24 h ROCK Inhibitor	
	$\alpha^*$ (-)	$\mu^{app}$ ( $10^{-2} \text{ h}^{-1}$ )
Results Member A	0.70 $\pm$ 0.24	2.44 $\pm$ 0.00
Results Member B	0.88 $\pm$ 0.09	2.42 $\pm$ 0.00

## ANNEX V

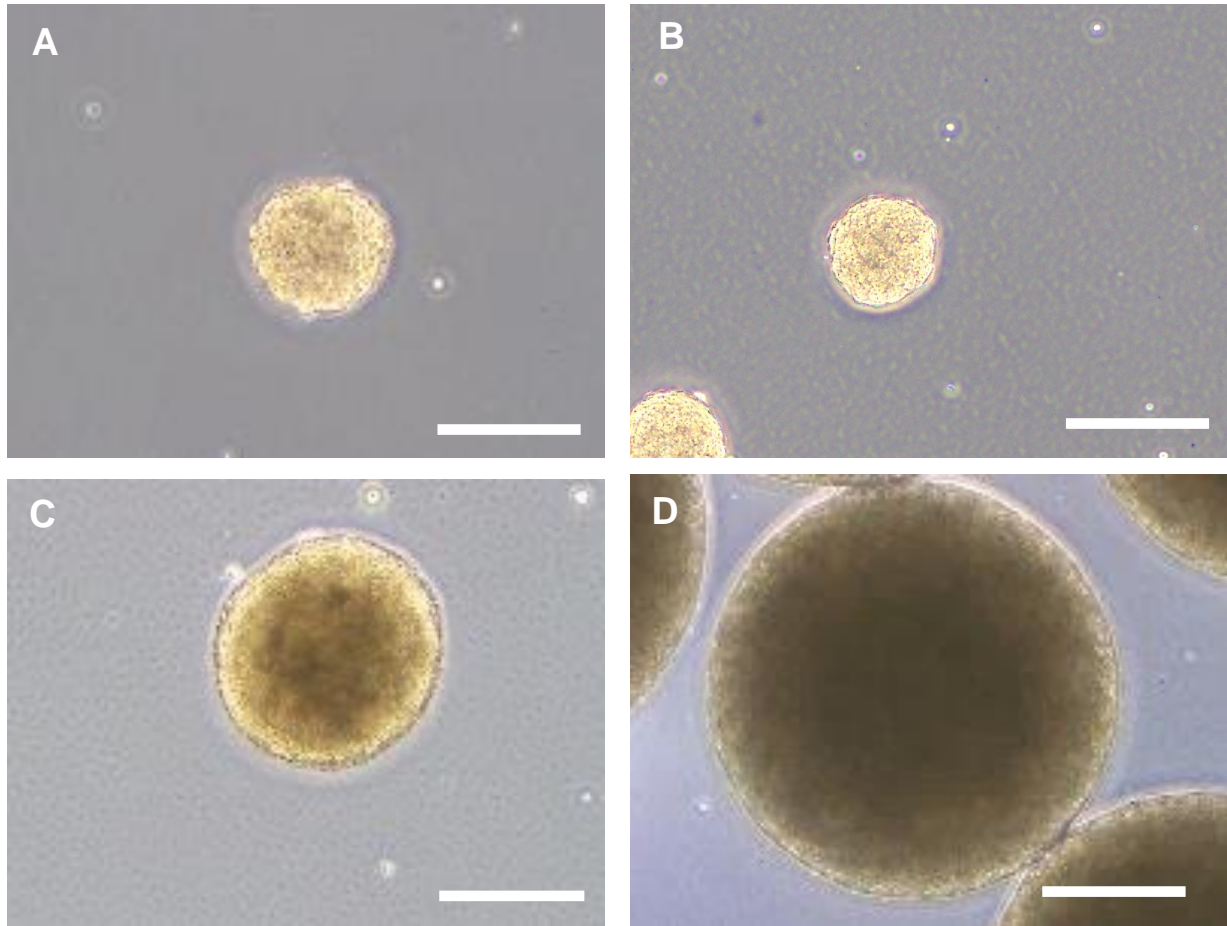


**Figure 21 - Phase contrast microscopy images of aggregates composed of Type A cells from the culture in a 30 mL bioreactor.** These images were taken at  $t = 24$  h, with the ROCK inhibitor present in the culture for **(A)** 24 hours and **(B)** 120 hours, and at  $t = 120$  h, with the ROCK inhibitor present in the culture also for **(C)** 24 hours and **(D)** 120 hours. These unpublished results were kindly provided by a laboratory member ( $n = 1$ ). (Scale bars = 200  $\mu\text{m}$ ).

